AD 642 159

TIME-DEPENDENT COMPRESSION PROPERTIES OF ALUMINUM ALLOY 2024-0 AT 500 F (533 K)

By

Ralph Papirno

Interim Technical Report ARA-290-4

31 October 1966

Prepared for

ARO-D Project No. 337
Contract No. DA31-124-ARO-D-337
U. S. Army Research Office, Durham
Duke Station
Durham, North Carolina

ALLIED RESEARCH ASSOCIATES, INC.
VIRGINIA ROAD · CONCORD, MASSACHUSETTS

Dedication

George Gerard

May 15, 1922 - June 14, 1966

It was a rare privilege to have been a collaborator of George Gerard. Among the gifts he gave to all of us who worked with him were his original ideas. These will serve as both inspiration and sustenance to us over the years to come. The world knew him as an outstanding research worker in the aeronautical and astronautical sciences; we knew him also as a teacher. In the things we do now we hope that there will always be a touch of the genius and the style of George Gerard.

This investigation on which we report here had its genesis in George's fertile imagination. As we continue the work we can only hope that we learned well all the things he taught us, and that we can achieve the objectives he set for us. It is altogether fitting, therefore, that we dedicate this work to its originator, George Gerard.

Ralph Papirno

Abstract

Compression creep and compression constant strain-rate tests were performed on thick wall cylindrical specimens of aluminum alloy 2024-0 at 500 F (533 K). Using the assumption that the equation of state of the material is a function only of stress, strain, and strain rate, the creep curves were analyzed to yield constant strain-rate, stress strain data. Comparisons between the creep-derived and the directly measured constant strain-rate data show that the data are not exactly equivalent but the discrepancies are sufficiently small so that to a first approximation the equation of state assumption can be considered valid.

The data presented will be utilized in the next stage of the investigation, to develop theoretical results for the Gerard Theory of Time Dependent Plastic Stability for comparison with experiments now in progress.

Time-Dependent Compression Properties of Aluminum Alloy 2024-0 at 500 F (533 K)*

I. Introduction

Our study of the time dependent plastic stability of structural elements is based upon an approach first stated by George Gerard in 1956 (Ref. 1) in which time dependent creep buckling was hypothesized to be predictable using plastic buckling formulas providing that the appropriate material property parameters were employed in the formulas. Later Gerard developed this hypothesis into a theory for the creep buckling of columns (Ref. 2), plates and shells (Ref. 3), and finally into a universally applicable approach for structural elements (Ref. 4). Simultaneously, Gerard and Papirno performed a series of experiments on columns (Refs. 5 and 6) and on plates (Refs. 7 and 8) which, despite small discrepancies, tended to support the theoretical results.

The development of the theoretical creep buckling solutions in quantitative form required tangent modulus data and plasticity reduction factors. These were derived graphically in a series of steps from the creep curves using a procedure which is described in some detail in Ref. 6. The key intermediate step on which the process depended was the derivation of a set of constant strain-rate stress-strain curves; it was from these that the necessary tangent modulus and plasticity reduction factor data were derived. It was implicitly assumed, in this development, that as a first approximation stress, strain, and strain rate were the governing parameters. At the time the theory was first developed there was some question as to the relationship between the constant-strain-rate stress-strain curves derived from the creep data and those which might be obtained directly from a specimen in a test. At the time the question arose, the equipment to perform the constant strain rate tests over the required range of strain rates was not available and a comparison could not be made.

An initial (but minor) objective of the current program was to determine whether the two types of constant-strain-rate stress-strain curves were equivalent

*English system units are used throughout this report followed by the appropriate International System (SI) metric units in parenthesis.

and whether they could be used interchangeably. If this were the case, then time-dependent plastic buckling based upon creep and buckling based upon the corresponding constant strain-rate loading would also be equivalent and only one set of material property data would be necessary for these two types of time-dependent buckling. As will be shown in this report, however, the data from the two types of test although not exactly equivalent are in relatively good agreement. Inferences on differences between the two types of buckling behavior, therefore, will be deferred until buckling tests have been completed.

One major specific objective of our current investigation is the study of the time dependent plastic buckling behavior of isotropic, circular, thin wall cylinders loaded in axial compression at elevated temperatures under constant stress (creep) and monotonically increasing stress (constant strain-rate). Mechanical property data are required for the development of the theoretical time-of-buckling predictions for each of the types of loadings. This report presents such mechanical property data, and in a subsequent report experimental buckling times of cylinders obtained from tests now in progress will be compared with theoretical predictions.

II. Experimental Program

Thick wall cylindrical specimens of aluminum alloy 2024-0 were tested in a pneumatically actuated testing machine. Both creep tests and constant-strain-rate stress-strain tests were performed at 500 F (533 K) in the same testing machine. The appropriate strain-time or stress-strain data were recorded autographically.

Specimens: The material chosen for this investigation was aluminum alloy 2024-0 which past experiments had shown to have well characterized elevated temperature compression properties. For the tests described here, 10ft. (3.05 m) lengths of 2.0 in (50.8 mm) O.D. and 0.12 in (3.0 mm) wall thickness drawn tubes of aluminum alloy 2024-T4 were cut into approximately 5.0-7.0 in (127-178 mm) sections for specimen blanks. The tubing lengths were numbered starting with unity and the individual specimen blanks were identified by a dash number following the length number (1-1, 1-2 etc.).

Only odd numbered blanks were used for the compression properties tests. The even numbered section were set aside for later use in buckling experiments. The cylindrical compression specimens were machined from the material in the T-4 condition to the dimensions shown in Fig. 1. Two pairs of gage marks, 2.0 in (50.8 mm) apart were made using a 0.0135 in (0.343 mm) diameter drill (No. 80 size) penetrating only 0.005 in (0.12 mm) into the specimen; these would accommodate the contact points of an Allied Research elevated temperature compressometer based upon the concentric tube arrangement.

It should be noted that all of the specimens tested met the tolerance specifications given in Fig. 1 and in many specimens, the thickness and taper variations were of the order of $\pm$ 0.0001 in (0.0025 mm) over the specimen length.

An annealing heat treatment was used to obtain the "O" condition as follows:

1) Two hours at 775 F (686 K)
2) Furnace cool to 400 F (477 K) at a maximum rate of 35 F (19.5 K)
3) Air cool to room temperature.

Testing Machine: All of the experiments were performed in an Allied Research Associates precision pneumatic testing machine equipped with a Marshall tubular testing furnace and Allied Research concentric tube elevated temperature compressometers having linear variable differential transformer (LVDT) sensors. The testing machine loading frame and temperature control console are shown in Fig. 2, while

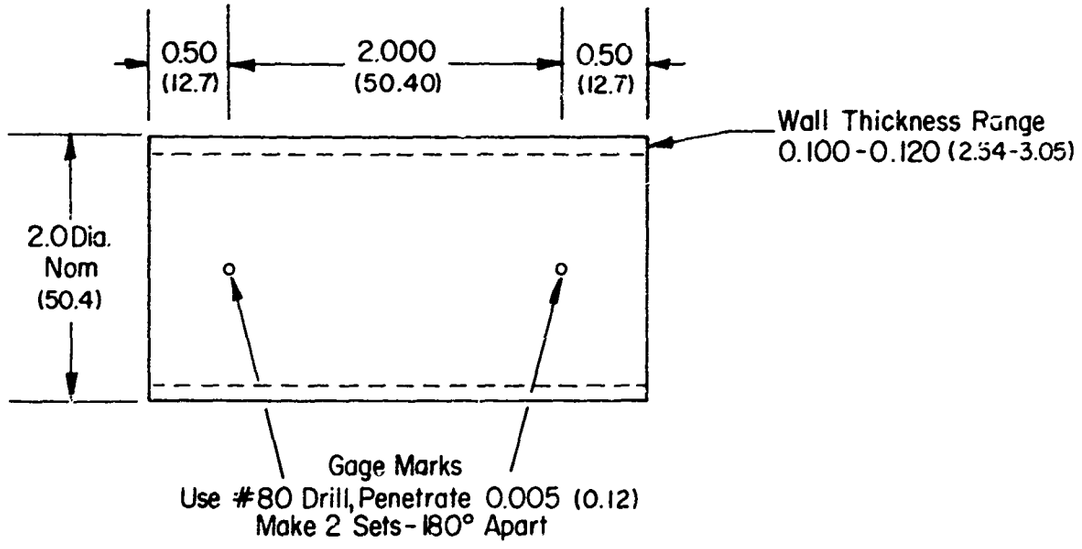

Dimensions in inches. Values in parenthasis are in millimeters.

NOTES:

1. OD & ID Concentric to ±0.0005 (±0.012) or better.
2. Taper no more than 0.0005/3.0 (.012/76)
3. Ends flat, square and parallel

Figure 1 Cylindrical compression specimen dimensions.

5922

the loading control console is shown in Fig. 3. Incorporated in the loading console is a pneumatic servo pressure regulator for maintaining constant load. An Allied Research ramp function generator and electro-pneumatic servo system which operates using the compressometer output achieves constant strain-rate loading. This latter is on the "Servo Controller" panel in the console shown in Fig. 3. The testing machine is used in the horizontal position shown in Fig. 2 to minimize temperature gradients caused by the chimney effect which would be present in a vertical installation.

Autographic Recording System: All of the data were recorded autographically on an X-Y Recorder shown in Fig. 3. For the creep tests, the stress-strain behavior as the creep load was being applied was recorded as well as the strain-time creep data. During the constant strain rate tests stress-strain data were recorded.

Rational stress-strain units were obtained on the autographic recording by calibrating the system prior to each test. The source of the stress signal was an electric pressure transducer. The stress axis was calibrated using an integral pneumatic calibration system for each specimen before each test. The procedure consisted of adjusting the variable gain of the Y axis of the recorder, such that the pressure equivalent of a stress 1000 psi (6.89 N/mm^2) when applied to the transducer, resulted in a pen deflection of one major subdivision on "20 x 20 to the inch" graph paper.

The strain axis was calibrated using a micrometer screw, calibration jig installed in the specimen position on the testing machine. The variable gain of the X axis of the recorder was adjusted so that a micrometer deflection of 0.020 in (0.51 mm) resulted in a recorder deflection of ten major chart paper subdivisions. This is the equivalent of 1000 micro-in/in (1000 micro-cm/cm) per major subdivision. The jig is shown in the calibration position in Fig. 4.

The timing signals for the creep test originated in an 8 hour-period sawtooth timing generator. The output of this generator was applied to the Y axis of the recorder and the variable gain was adjusted so that the recorder deflection for one-half cycle (4 hrs) was six one-inch subdivisions on "20 x 20 to the inch" chart paper. This is the equivalent of 2 minutes per smallest subdivsion. The repetitive sawtooth allowed the monotonically increasing strain data curve to be folded back upon itself electrically so that many hours of recording would be contained on one notebook size sheet of graph paper.

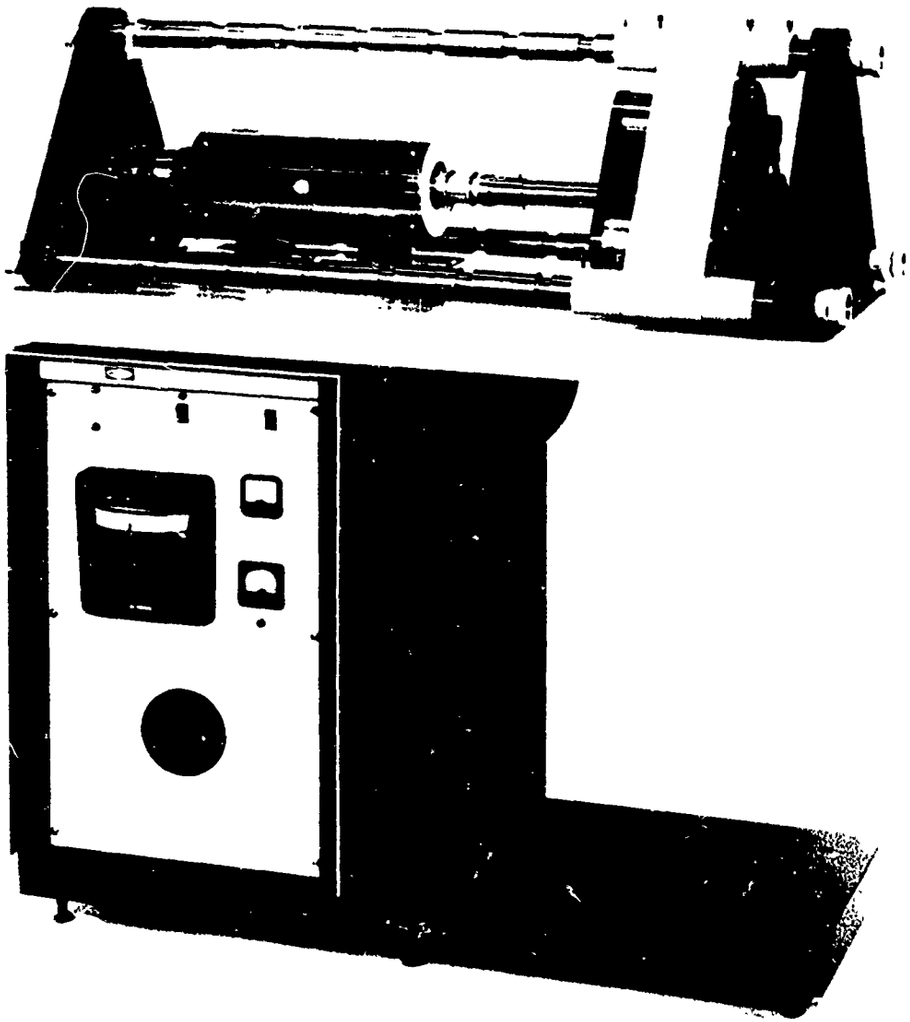

Figure 2 Testing Machine Loading Frame and Temperature Control Console

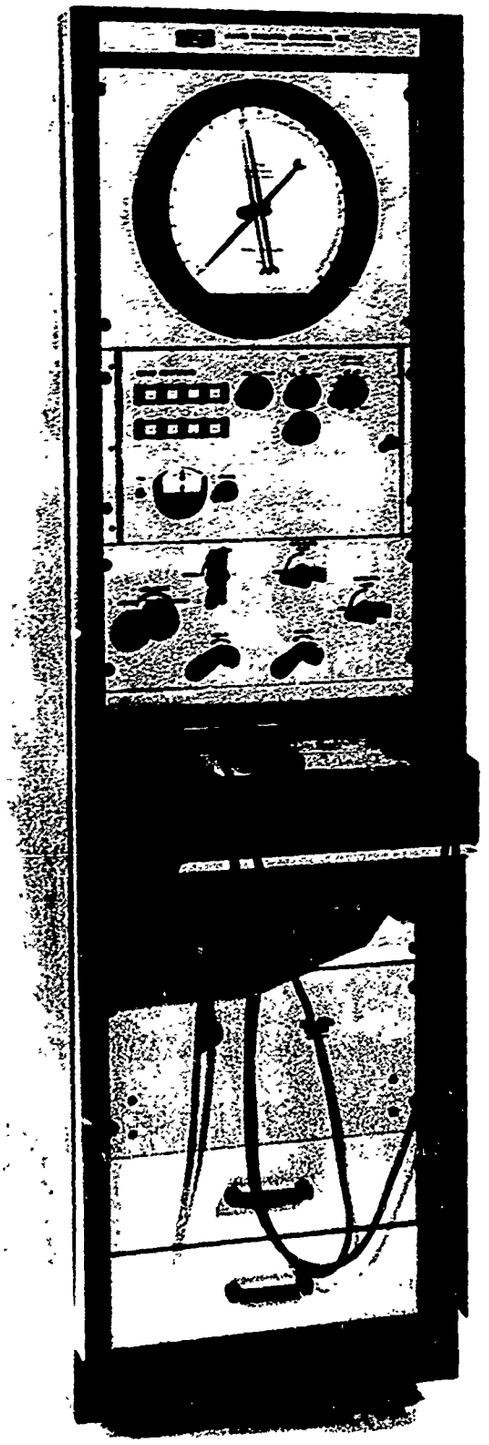

Figure 3 Load Control Console Containing Constant Strain-rate Servocontrol System

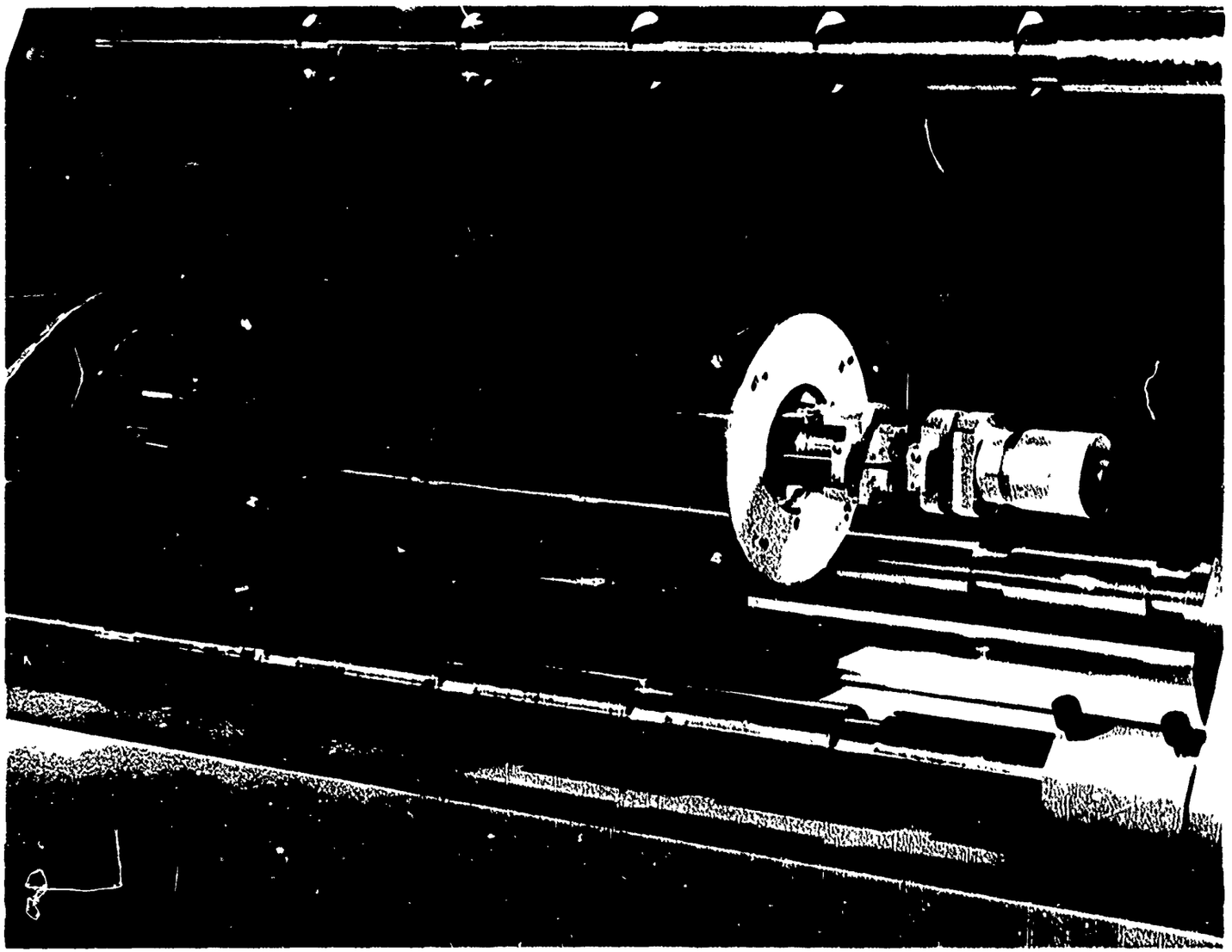

Figure 4 Strain Calibration Jig

A typical strain-time record is shown in Fig. 5 for a creep test at 500 F (533 K) on an aluminum alloy thick wall cylindrical specimen. The stress-strain behavior of the specimen during the application of the creep load has also been shown. A typical record from a long time constant-strain rate test on the specimen material at 500 F (533 K) and at a strain rate of 100 micro-in/in (100 micro-cm/cm) is shown in Fig. 6.

Experimental Procedure: After the specimen dimensions had been measured by micrometer and the autographic system had been calibrated, the specimen was installed between the testing machine furnace rams and then centered. A spherical seat on one of the ram ends was adjusted so that there was uniform contact between the specimen ends and the ram seats. A small load was applied to the specimen to retain it in position.

Next, two thermocouples were installed and held in contact with the specimen surface at a midpoint location by spring loaded fiberglass ribbons as shown in Fig. 7. One thermocouple was in the temperature using a standard potentiometer readout. The concentric tube compressometers (one on each side of the specimen) were next installed with their contact points in the small predrilled shallow holes which established the two-inch gage length. Inconel-X coil springs retained the contact points on the specimen. It should be noted that the two compressometers were not mechanically coupled. Separate measurements were made on each side and averaged electrically for recording, and also for the control system signal in the constant strain rate tests.

The specimen was heated to 500 F (533 K) and held for one-half hour at temperature before testing. If a creep test were scheduled, the autographic system was set up to record the stress-strain behavior during the application of the creep load. Then the creep strain record was obtained, either by stopwatch and observation for very short time tests, or by the substitution of the stress signal by the sawtooth timing signal for longer time tests. This latter procedure produced a record similar to that shown in Fig. 5. For the constant strain rate test, the controls were set to obtain the proper strain rates, the servo system was balanced, and the test was initiated by pressing a button. This energized the ramp function generator which served as the strain rate reference and which combined with the compressometer signal to form the error signal for the servo.

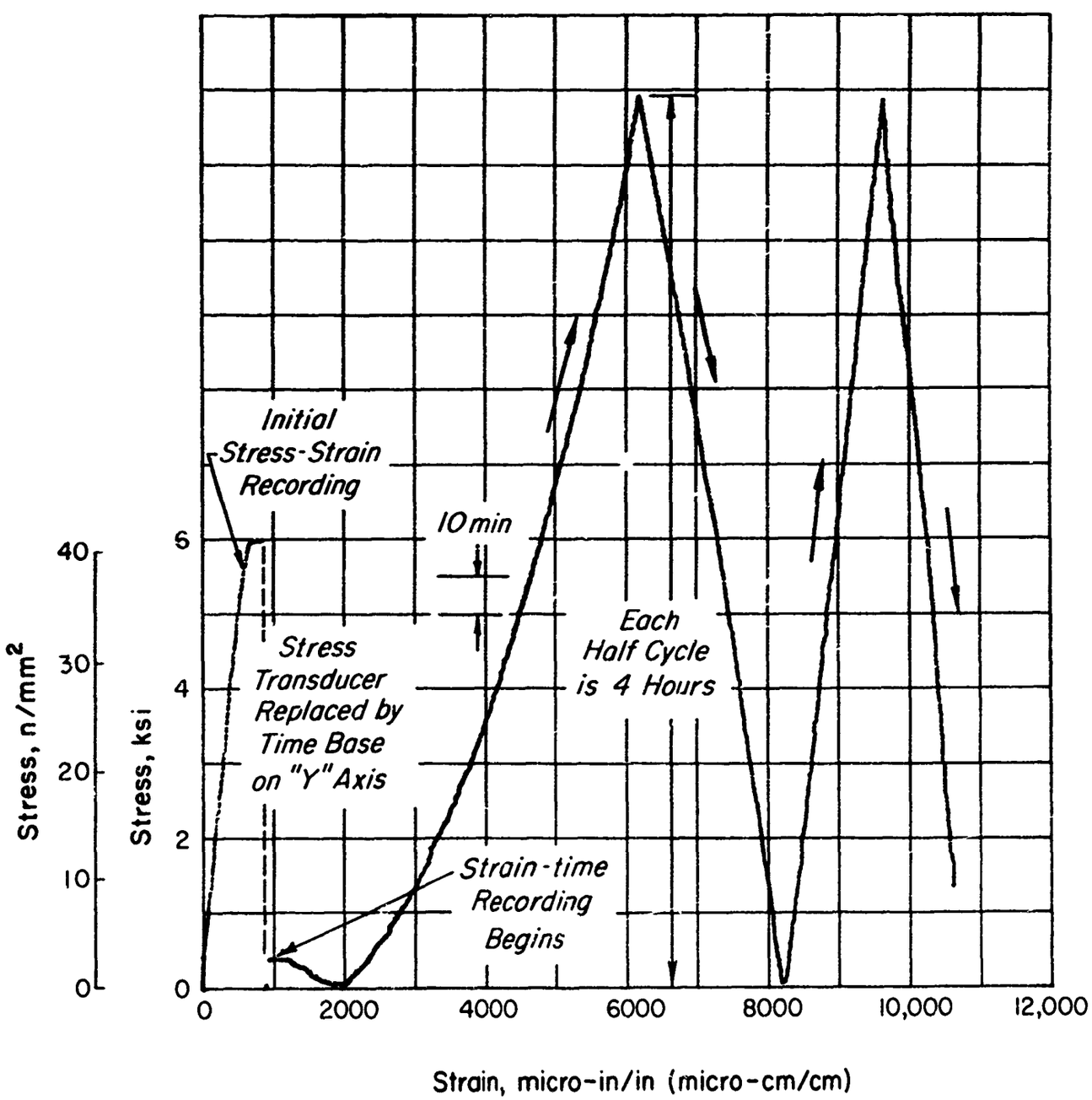

Figure 5 Autographic recording for a compressive creep test on aluminum alloy 2024-0 at 500° F (533° K) and 6000 psi (41.2 N/mm^2) applied stress.

547

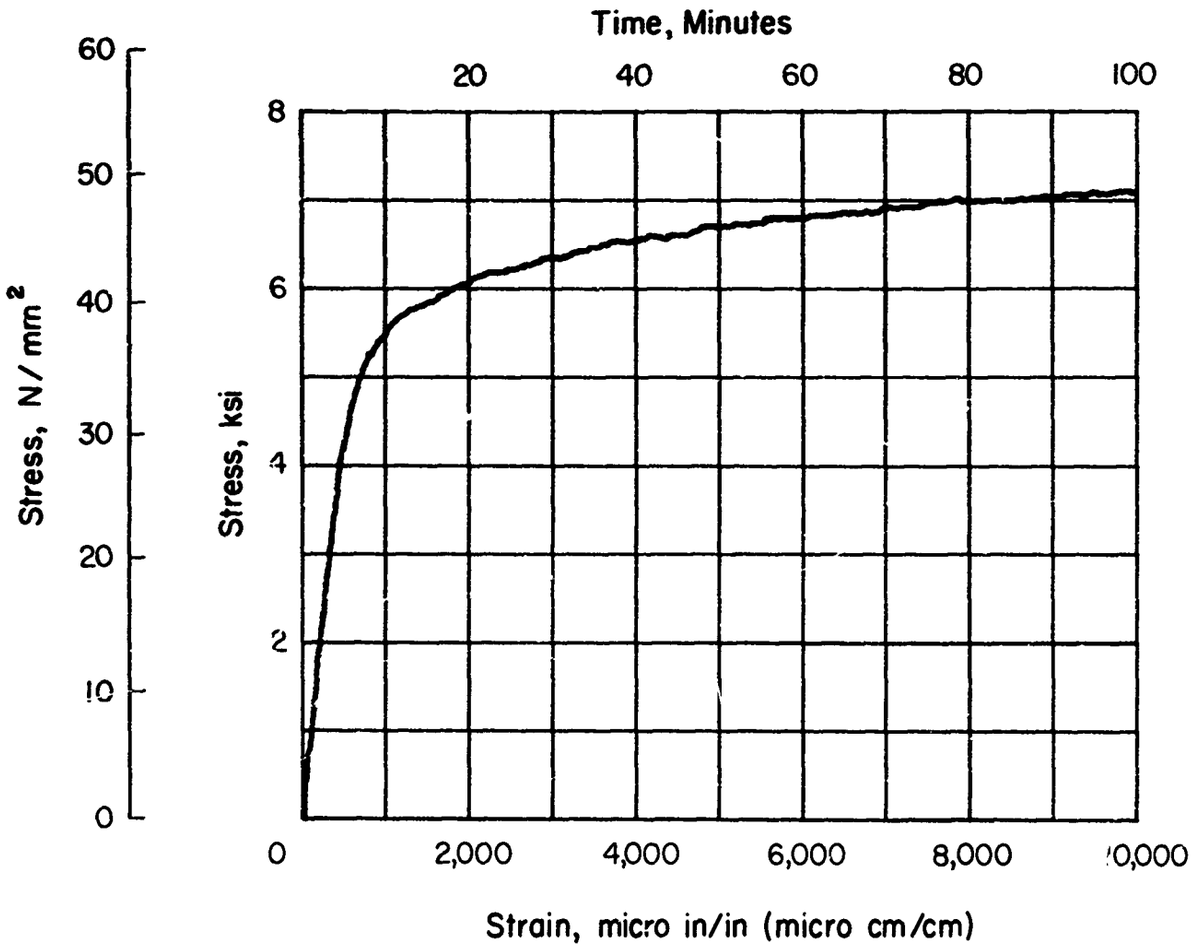

Figure 6 Autographic recording for a compressive constant strain-rate test on aluminum alloy 2024-0 at 500°F (533° K) and 100 micro-in/in (100 micro-cm/cm) strain rate

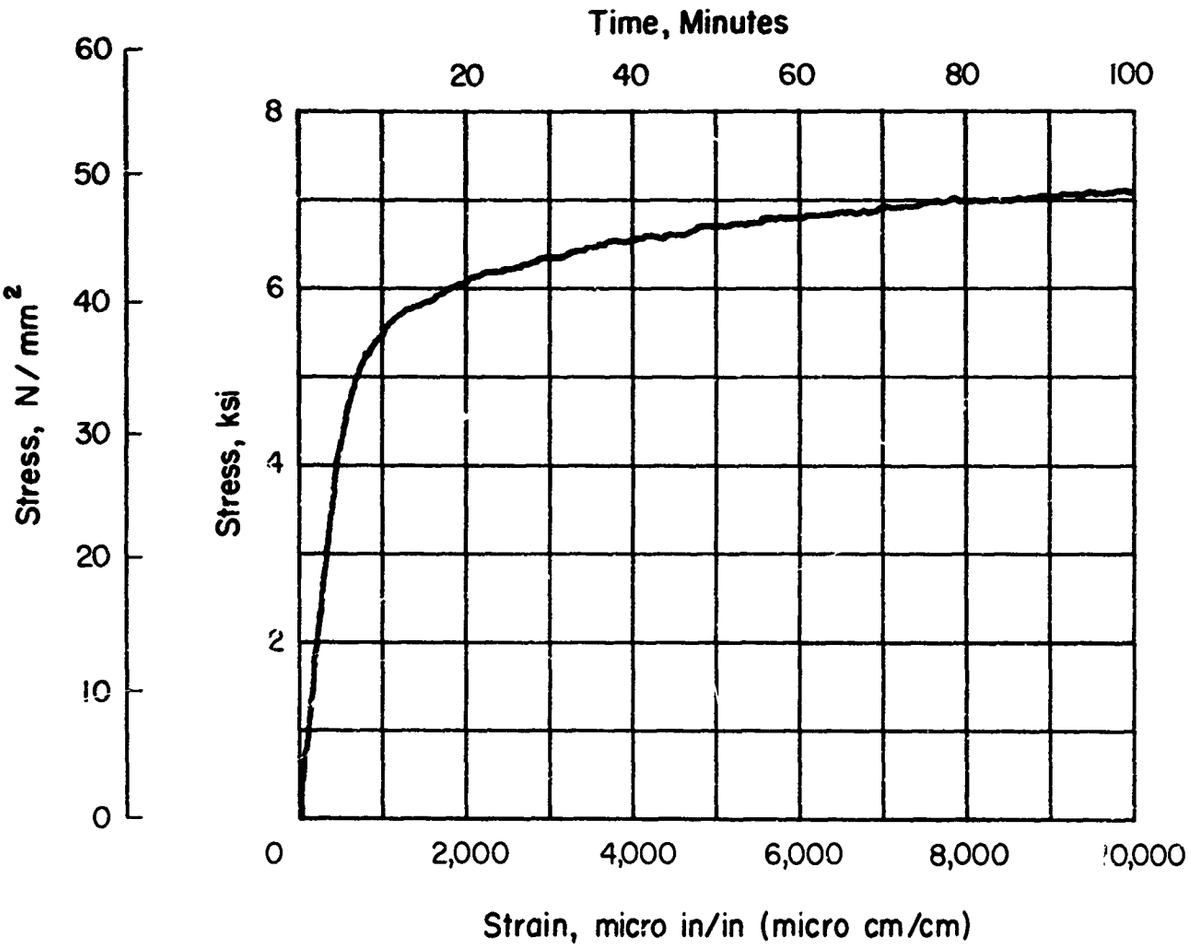

Figure 6 Autographic recording for a compressive constant strain-rate test on aluminum alloy 2024-0 at 500°F (533° K) and 100 micro-in/in (100 micro-cm/cm) strain rate

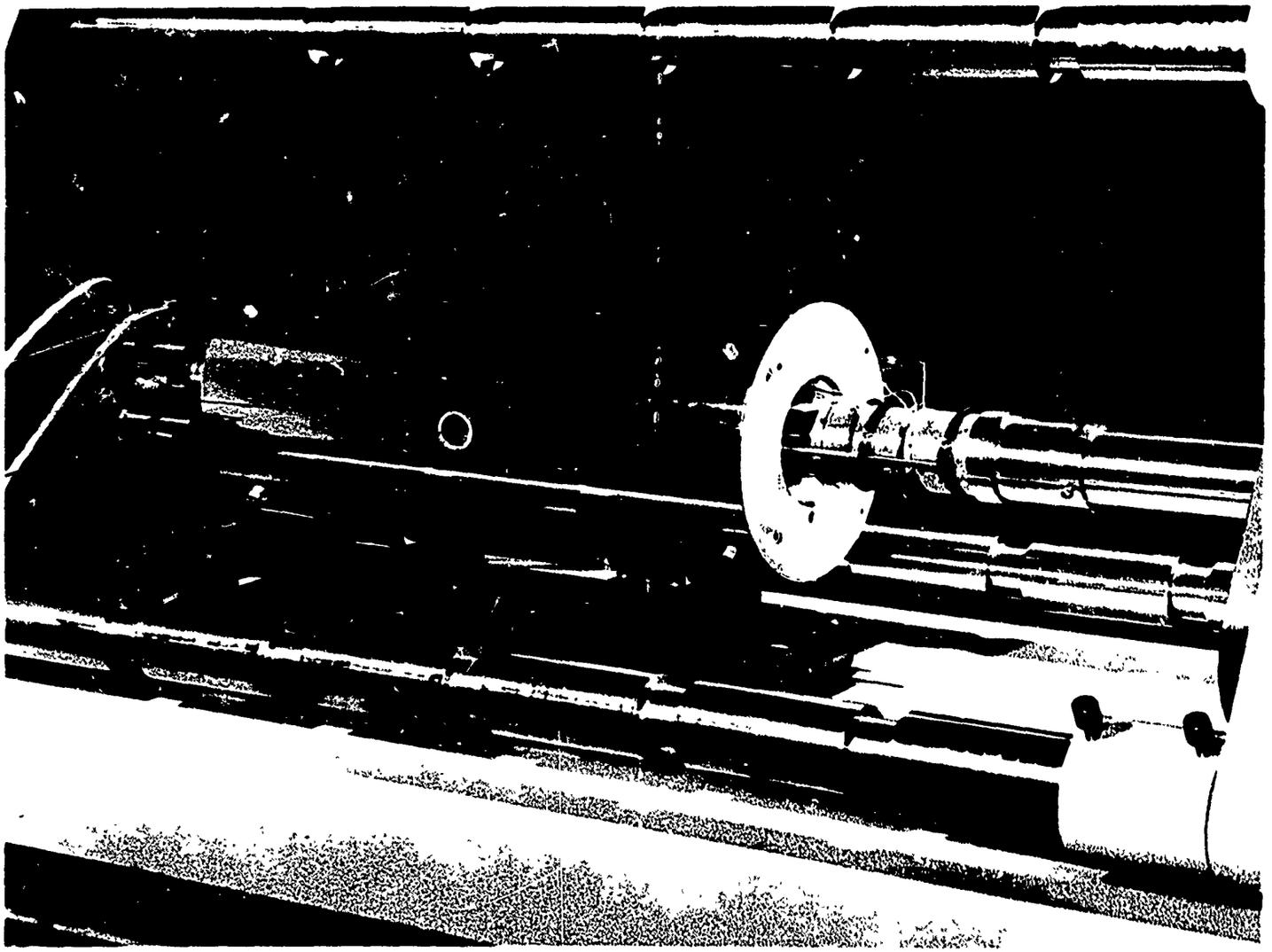

Figure 7 Specimen shown in Position in Testing Machine with Thermocouples and Compressometers Installed

Experimental Accuracy: This system of individual calibration of stress and strain before each test tended to minimize experimental errors in the autographic data. Because of non-linearities in the LVDT's a maximum error of $\pm$ 1% is possible in the strain signal while the stress signal error is the order of the recorder line thickness-equivalent to a stress of 50 psi (0.34 N/mm^2).

Temperature errors were comparably small. The horizontal testing arrangement minimized chimney effects in the furnace with the result that the spatial variation of temperature in the gage length was found to be approximately $\pm$ 1 F ($\pm$ 0.6 K). Temporal variations of temperature during the test times were less than $\pm$ 1 F ($\pm$ 0.6 K).

There was a possible error from small changes in load during the creep tests caused by drift in the pneumatic servo control pressure regulator valve. These changes could induce a change in stress in the specimen of the order of 10 psi (0.07 N/mm^2).

Scatter is a characteristic of creep data. It has been difficult in the past to assign a specific cause to creep data scatter, or to determine how much can be attributed to small variations in the environmental parameters and how much is inherent in the material response itself. In creep tests small undetermined variations in the temperature, indeterminate stress concentrations at the loaded edge, thermal stress within the specimen, and other mechnical and thermal conditions can all differ from one specimen to the next. Grain size variations, non-homogeneities in composition and other material parameters which vary among the specimens also contribute to scatter. All of these variations are in the tenth-of-one-percent order of magnitude or less, yet in the relatively long times of a creep test they may give rise to large variations in creep strain.

On the other hand in controlled strain-rate testing such scatter of the data is rare since it would be manifested by variations in stress. In the plastic region of the stress-strain curve small variations in strain or temperature would have little effect on stress. Hence the stress in these tests is a relatively non-sensitive parameter. As a result the repeatability of the constant strain-rate data is good.

III. Experimental Data

The experimental data presented herein were reduced from autographic records such as those shown in Figs. 5 and 6. A catalogue of the specimens tested with their dimensions is given in Table 1 in the Appendix. The individual data curves for each of the specimens tested are also given in the Appendix. The averaged raw data as well as the analyzed data obtained from the average curves are given in this section of the report. These data are presented in two categories pertinent to either the creep tests or to the constant strain-rate tests.

Malfunction of the heat treating furnace caused incomplete annealing to the "O" condition in some of the specimens in the first heat. This was determined by hardness testing of the heat treated tubes. As a result the data from all 15 specimens in this heat were discarded and are not reported herein. The tests were repeated, however, with properly treated material.

Creep Test and Related Data

A typical creep test is conducted under two loading regimes: a) the initial application of load and b) the constant load phase. The initial load application is equivalent to a short time stress-strain test which in our apparatus, was performed at approximately constant loading rate of the order of 40,000 psi/min (276 N/mm^2/min). It was appropriate to conduct short time tests for these conditions and the averaged data for three such test is shown in Fig. 8. The individual curves for each of three tests which were averaged to obtain Fig. 8 are given in the Appendix.

Creep tests were conducted at the following stress-levels:

8400 psi (57.8 N/mm^2)
8000 psi (55.1 N/mm^2)
7840 psi (54.0 N/mm^2)
7500 psi (51.7 N/mm^2)
7000 psi (48.2 N/mm^2)
6500 psi (44.8 N/mm^2)
5500 psi (37.9 N/mm^2)

The averaged data for each of the stress levels is shown in Fig. 9, while the individual curves for each of the stress levels are given in the Appendix.

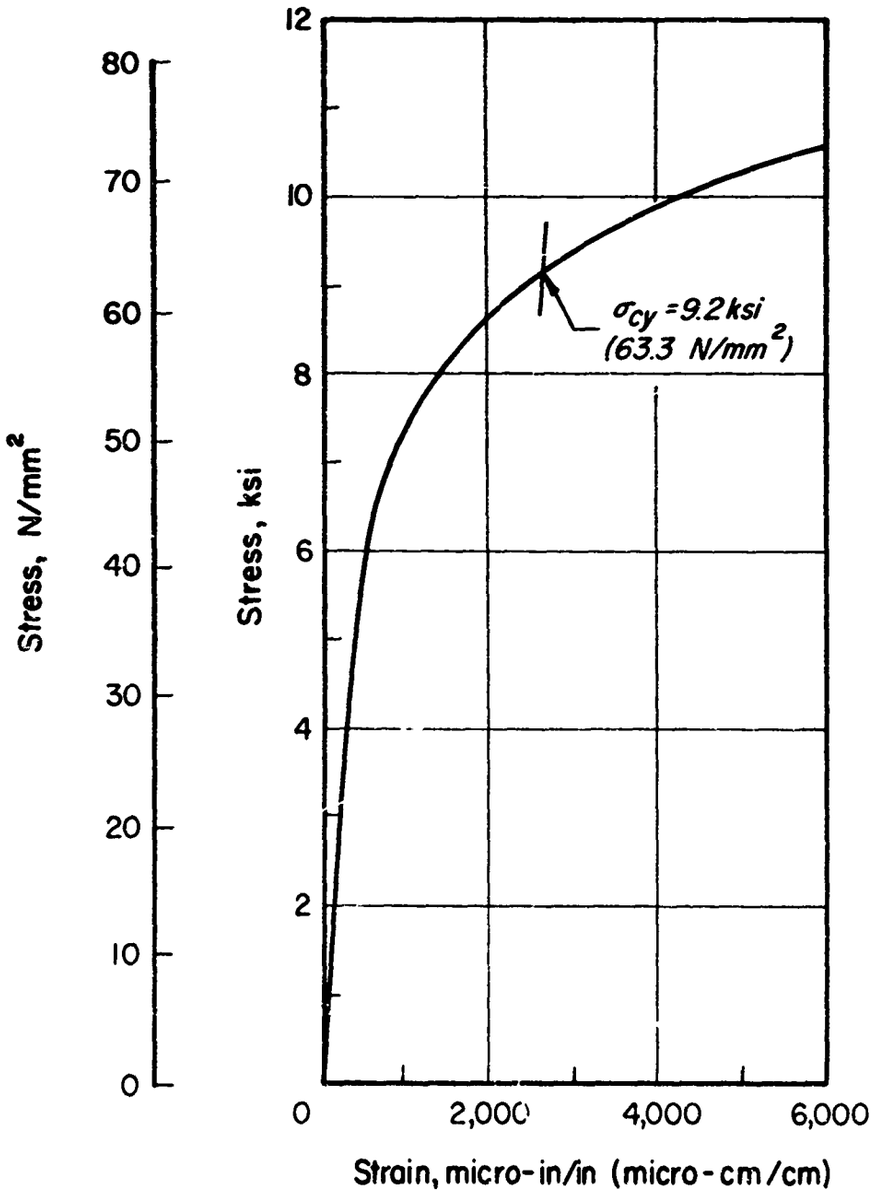

Figure 8 Average short time stress-strain data simulating the application of load in a creep test. Stress rate approximately constant at 40,000psi/min (276 N/mm^2). Aluminum alloy 2024-0 at 500° F (533° K).

5933

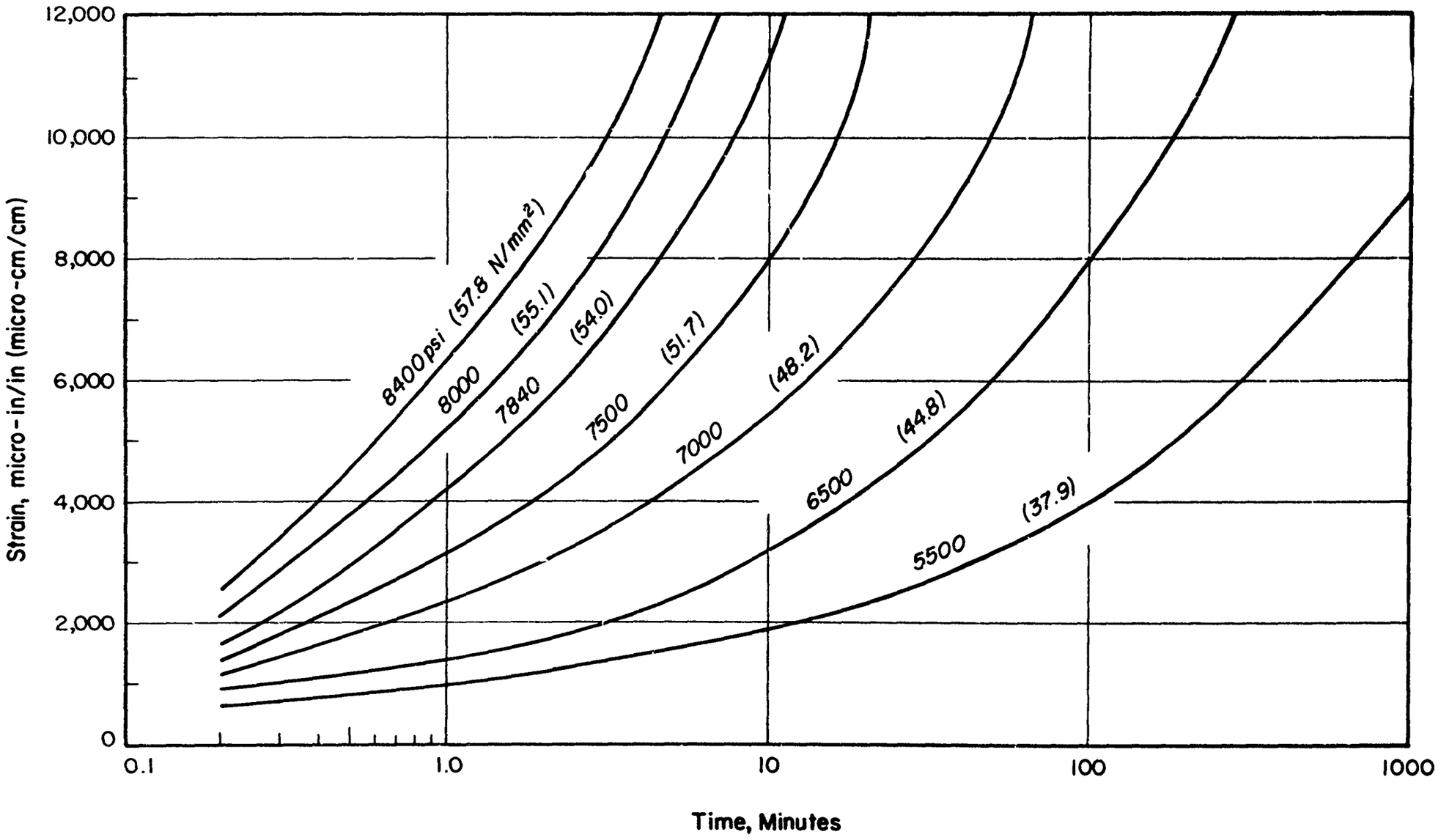

Figure 9 Average creep curves for aluminum alloy 2024-0 at 500° F (533° K).

Constant Strain-Rate Stress-Strain Data

A set of average stress-strain curves from tests at a variety of strain rates are shown in Fig. 10. The individual data curves for each of the tests are given in the Appendix for each of the following strain rates:

1000 micro-in/in/min	(1000 micro-cm/cm/min)
500 micro-in/in/min	(500 micro-cm/cm/min)
200 micro-in/in/min	(200 micro-cm/cm/min)
100 micro-in/in/min	(100 micro-cm/cm/min)
50 micro-in/in/min	(50 micro-cm/cm/min)
20 micro-in/in/min	(20 micro-cm/cm/min)

Analysis of Creep Data

The tangent at any given point on a creep curve represents an instantaneous value of strain rate for that curve. If the assumption is made that as a first approximation, the equation of state of a material can be expressed only as a function of stress, strain, and strain-rate, then graphical differentiation of a set of creep curves should result in a set of stress, strain, and strain-rate data. From these derived data an approximate set of constant strain-rate stress strain curves should be obtainable. This type of analysis, in which the effect of time is neglected, was performed on the creep curves.

In this data analysis, the average creep curves were first plotted in Cartesian coordinates, rather than in the semi-logarithmic form shown in the figures. These curves were then graphically differentiated to obtain stress-strain data points corresponding to the strain-rates used in the constant strain-rate tests and enumerated in the previous section. The set of derived constant strain-rate, stress-strain curves is shown in Fig. 11 for strain rates in the range 1000 micro-in/in/min to 50 micro-in/in/min (1000 micro-cm/cm/min to 50 micro-cm/cm/min). It was not possible to obtain a sufficient number of points to prepare a curve for 20 micro-in/in/min (20 micro-cm/cm/min).

Indirect and Direct Constant Strain-Rate Data

It is now possible to compare the approximate constant strain rate data obtained indirectly from the creep curves with data obtained directly from constant strain-rate tests. Sets of the two types of data for strain rates from 1000 micro-in/in/min to 50 micro-in/in/min (1000 micro-cm/cm/min to 50 micro-cm/cm/min) are shown in Figs. 12-16. It is clear from the figures that the two types of data

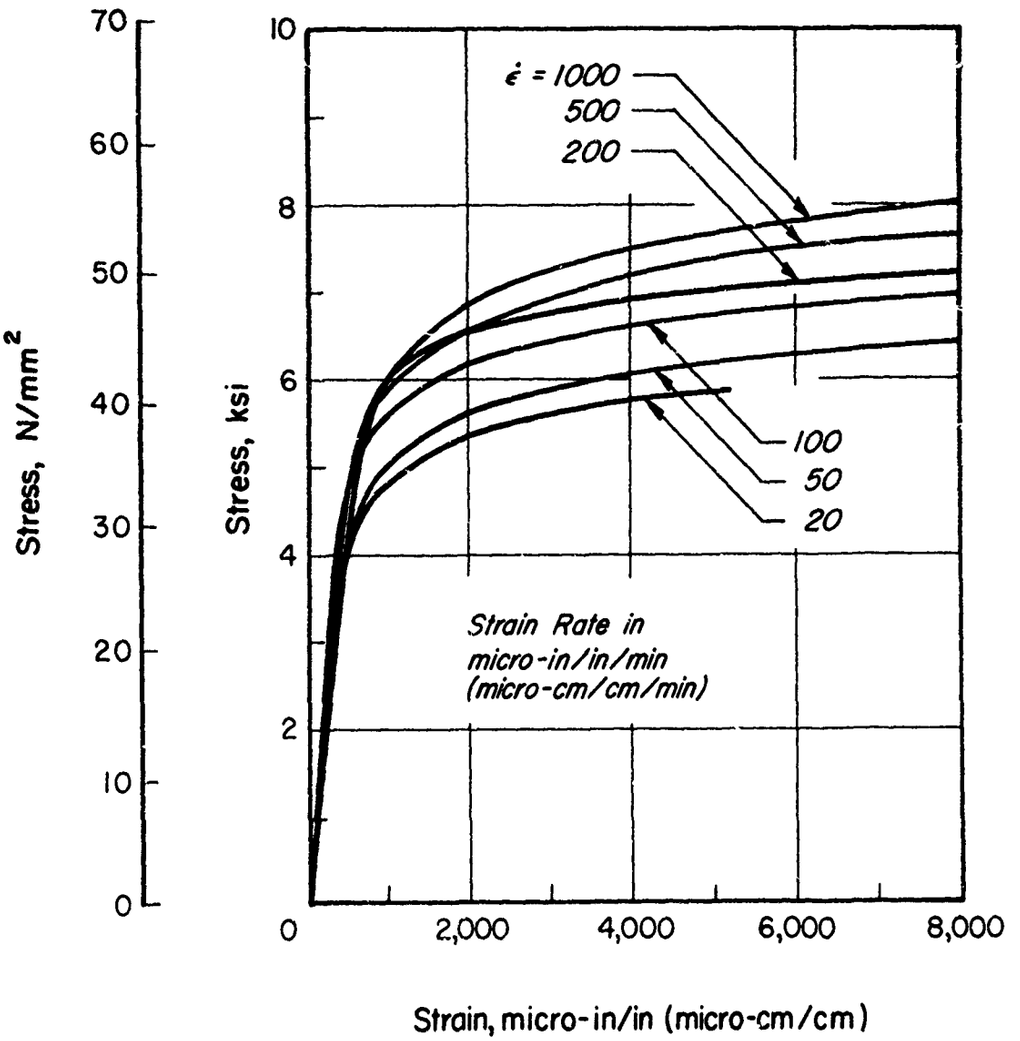

Figure 10 Average constant strain-rate, stress-strain curves as obtained directly from autographic recordings of constant strain-rate tests of aluminum alloy 2024-0 at 500° F(533° K).

5934.0

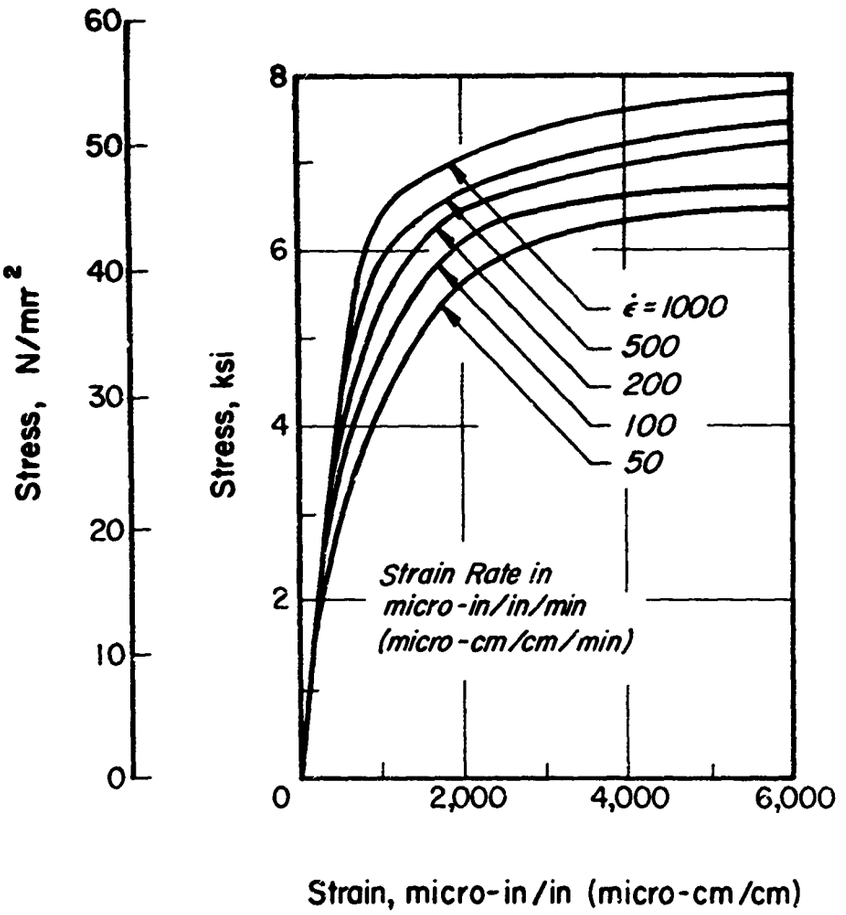

Figure 11 Derived average constant strain-rate, stress-strain curves as obtained from an analysis of data from creep tests of aluminum alloy 2024-0 at 500° F (533° K).

5946

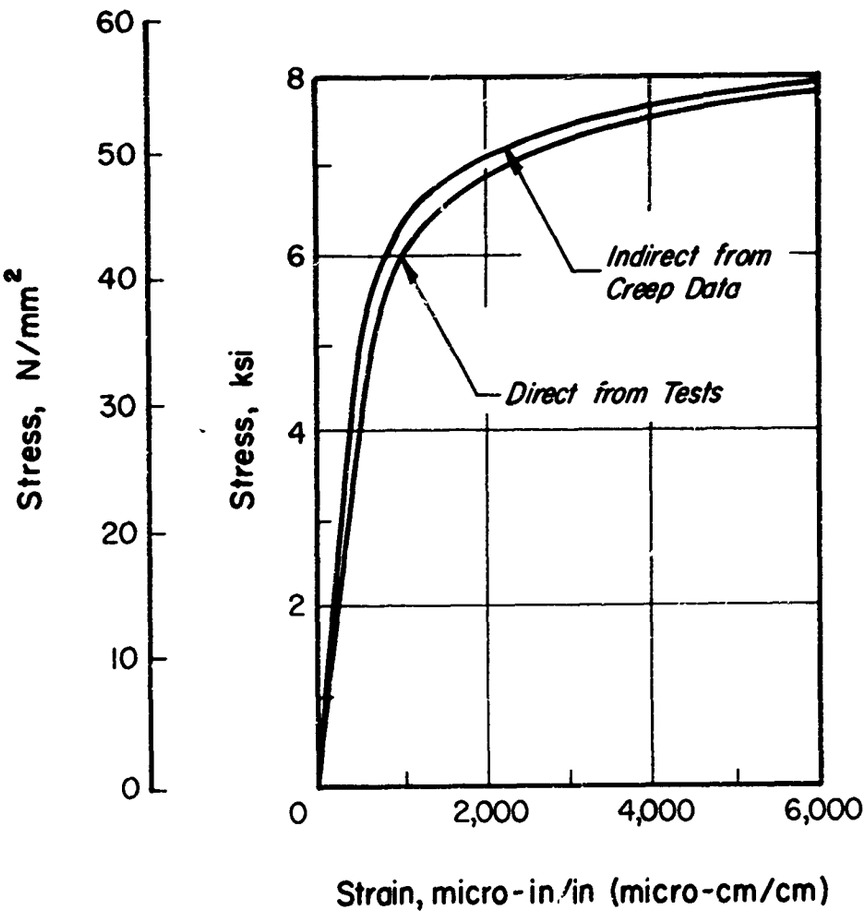

Figure 12 Comparison of indirect and direct constant strain-rate, stress-strain curves for 1000 micro-in/in/min (1000 micro-cm/cm/min) in aluminum alloy 2024-0 at 500° F(533° K).

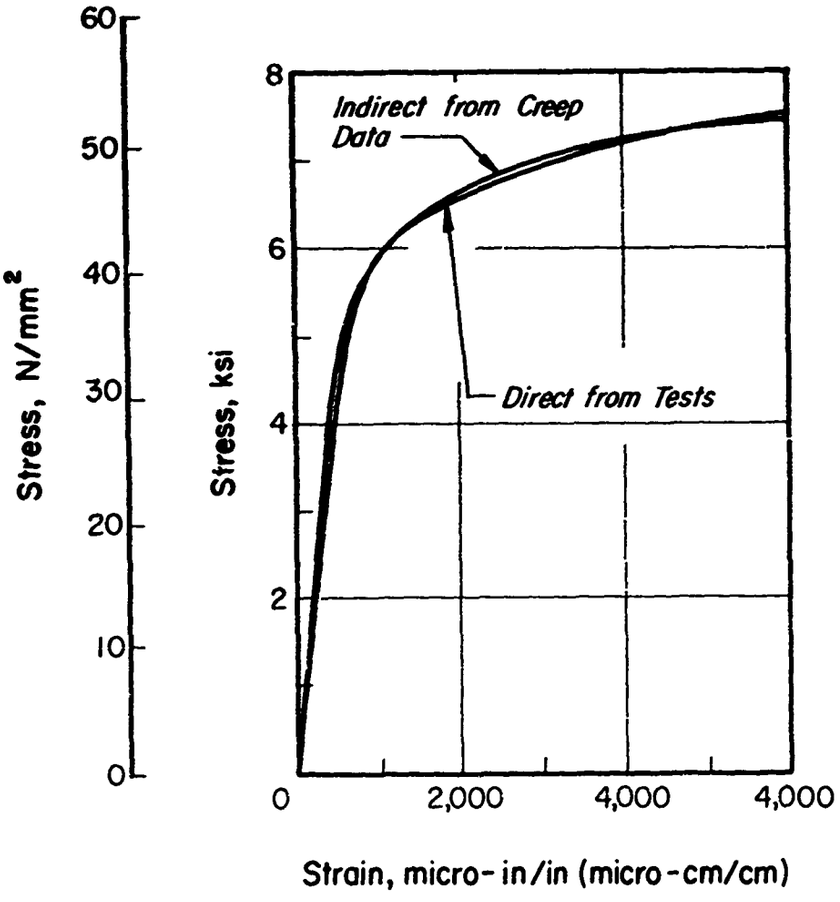

Figure 13 Comparison of indirect and direct constant strain-rate, stress-strain curves for 500 micro-in/in/min (500 micro-cm/cm/min) in aluminum alloy 2024-0 at 500°F (533° K).

5942

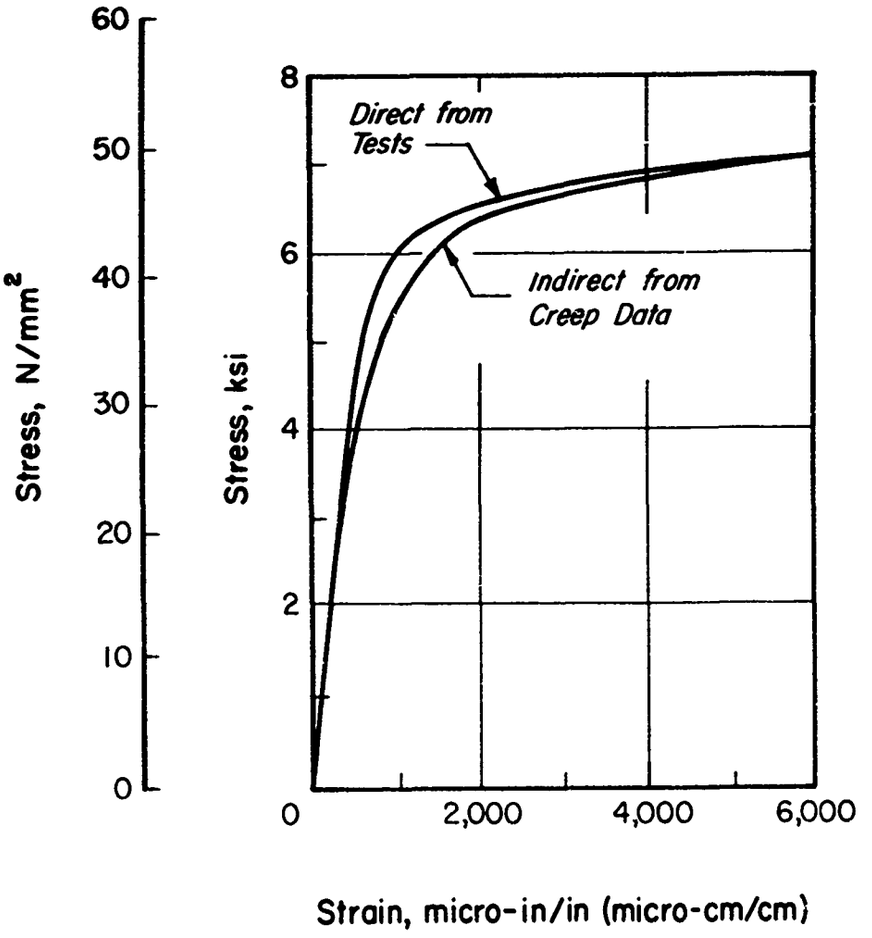

Figure 14 Comparison of indirect and direct constant strain-rate, stress-strain curves for 200 micro-in/in/min (200 micro-cm/cm/min) in aluminum alloy 2024-0 at 500° F (533° K).

5943

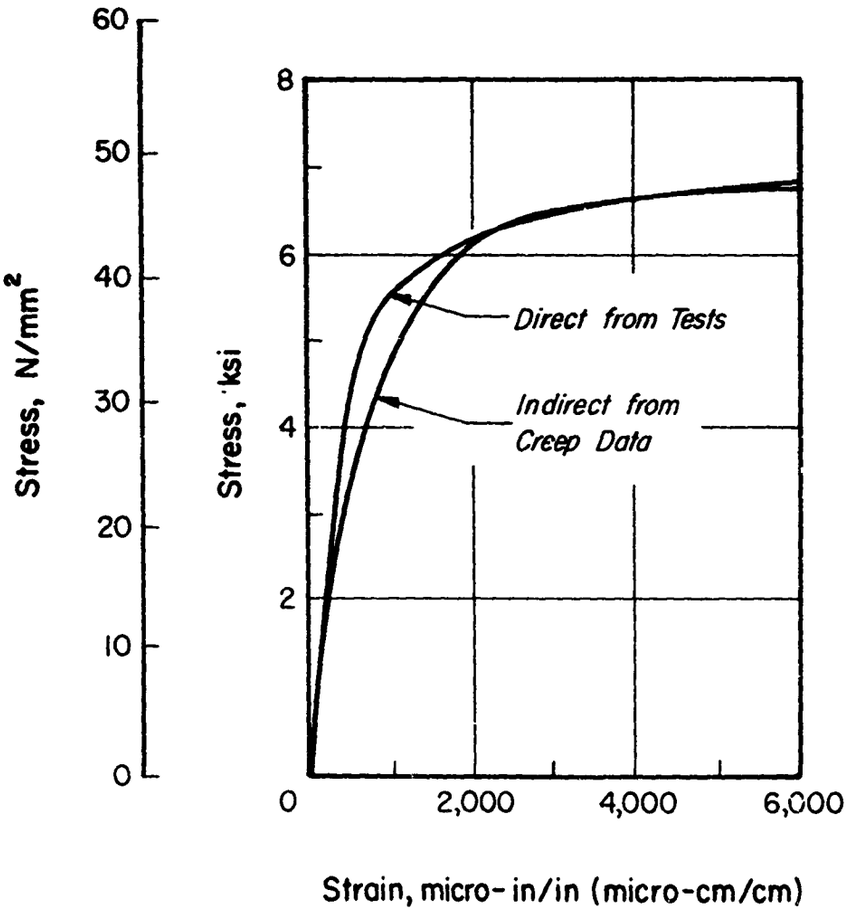

Figure 15 Comparison of indirect and direct constant strain-rate, stress-strain curves for 100 micro-in/in/min (100 micro-cm/cm/min) in aluminum alloy 2024-0 at 500° F (533° K).

5944

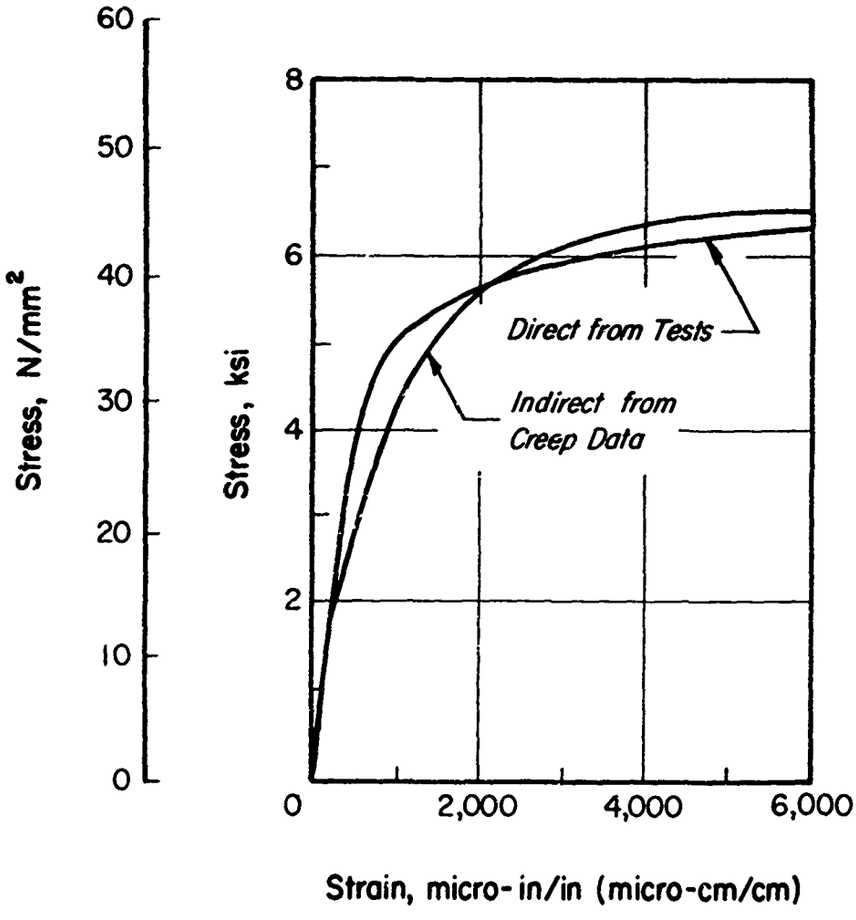

Figure 16 Comparison of indirect and direct constant strain-rate, stress-strain curves for 50 micro-in/in/min (50 micro-cm/cm/min) in aluminum alloy 2024-0 at 500° F (533° K).

5945

are not exactly equivalent. It is not possible at this time to assess the effect of the discrepancies between the two types of data in terms of our objective of using these data interchangeably for buckling time predictions. We will hold this assessment in abeyance until we have completed scheduled buckling experiments on cylinders using the two types of loadings.

Discussion of Results

It was not unexpected that constant strain-rate data derived from the creep curves would not exactly agree with data obtained directly from constant strain-rate testing. The agreement between the two types of data, as shown in Figs. 12-16, is close enough to conclude that an equation of state which is a function of stress, strain, and strain-rate is a good approximation to the behavior of the aluminum alloy material at 500 F (533 K) under the conditions tested.

V. Conclusions

The Gerard theory of time dependent plastic buckling of structural elements postulates that the form of relation for buckling prediction is that used for short-time plastic buckling. However, such material parameters as are required in the buckling relation are obtained from a set of stress-strain curves which are characteristic of the proposed loading history and which are obtained directly or indirectly from material property tests performed under the appropriate conditions.

In terms of the application of the results of test reported herein to develop the results of the Gerard theory the following major conclusions are drawn:

1) Constant strain-rate, stress strain properties of aluminum alloy 2024-0 at 500 F (533 K) obtained indirectly from creep tests are only slightly different from those obtained directly from controlled strain-rate tests.

2) The differences between the stress-strain properties obtained from the two types of tests are sufficiently small, that as a first approximation, the two types of data may be considered equivalent. The implication of this observation is that as a first approximation the equation of state of aluminum alloy 2024-0 at 500 F (533 K) can be considered to be a function of stress, strain, and strain rate.

Acknowledgment

The author wished to acknowledge the contributions of Mr. Joseph Furtado who assisted in the performance of the tests and Mr. Charles Lawnicki who manufactured the remarkably uniform test specimens.

Special thanks are due to Dr. Herbert Becker who reviewed the manuscript and made a number of valuable suggestions for its improvement.

V. References

1. Gerard, G., "A Creep Buckling Hypothesis," Journal of the Aeronautical Sciences, Vol. 23, No. 9, pp. 879-883, September 1956.

2. Gerard, G. and Papirno, R., "Investigation of Creep Buckling of Columns and Plates, Part 4: Column Creep Buckling Theory and Correlation with Experiments," WADC TR 59-416, Part IV, May 1961.

3. Gerard, G., "Theory of Creep Buckling of Perfect Plates and Shells," Journal of the Aerospace Sciences, Vol. 29, No. 9, pp. 1087-1090, September 1962.

4. Gerard, G., "A Unified Theory of Creep Buckling of Columns, Plates and Shells," Proceedings of the International Council of the Aeronautical Sciences, Third Congress, Stockholm - 1962, Spartan Books Inc., Washington, D. C., 1964, pp. 887-901.

5. Papirno, R. and Gerard, G., "Investigation of Creep Buckling of Columns and Plates, Part 3: Creep Buckling Experiments with Columns of 2024-0 Aluminum Alloy," WADC

6. Gerard, G. and Papirno, R., "Classical Columns and Creep," Journal of the Aerospace Sciences, Vol. 29, No. 6, pp. 680-688, June 1962.

7. Papirno, R. and Gerard, G., "Correlation of Plate Creep Buckling Theory with Experiments on Long Plates of Aluminum Alloy 2024-0 at 500° F, ASD-TDR-62-865, September 1962.

8. Papirno, R. and Gerard, G., "Creep Buckling of Plates: Experiments on Aluminum Alloy at 500° F," AIAA Journal, Vol. 1, No. 9, pp. 2127-2133, September 1963.

Appendix

Contained herein are the following:

1) Table 1. Specimen disposition and dimensions.

2) Figure 17: Results of all short time tests simulating the loading prior to creep.

3) Figures 18-24: Results of all creep tests.

4) Figures 25-30: Results of all constant strain-rate, stress-strain tests.

Table 1.

Specimen Disposition and Dimensions.

All Tests at 500K (533K) on

Aluminum Alloy 2024-0

Specimen Number	Test Type*	Outer Diameter in.	(mm)	Thickness in.	(mm)
2-11	ST	1.9950	(50.67)	0.1147	(2.91)
2-13	ST	1.9938	(50.64)	0.1142	(2.90)
2-17	ST	1.9932	(50.63)	0.1153	(2.93)
2-19	C-8.4	1.9924	(50.61)	0.1141	(2.90)
2-23	C-8.4	1.9943	(50.66)	0.1150	(2.92)
2-21	C-8.0	1.9936	(50.64)	0.1140	(2.90)
3-1	C-8.0	1.9943	(50.66)	0.1150	(2.92)
3-3	C-7.84	1.9934	(50.63)	0.1150	(2.92)
3-7	C-7.84	1.9919	(50.59)	0.1137	(2.89)
3-9	C-7.5	1.9940	(50.65)	0.1150	(2.92)
3-13	C-7.5	1.9938	(50.64)	0.1148	(2.92)
3-15	C-7.5	1.9951	(50.68)	0.1159	(2.94)
3-17	C-7.0	1.9937	(50.64)	0.1141	(2.90)
3-19	C-7.0	1.9915	(50.58)	0.1121	(2.85)
3-21	C-7.0	1.9968	(50.72)	0.1131	(2.87)
3-23	C-6.5	1.9968	(50.72)	0.1148	(2.92)
4-1	C-6.5	1.9975	(50.74)	0.1150	(2.92)
4-9	C-5.5	1.9977	(50.74)	0.1153	(2.93)
4-11	C-5.5	1.9939	(50.65)	0.1151	(2.92)
4-13	C-5.5	1.9954	(50.68)	0.1168	(2.97)
4-15	SR-1000	1.9975	(50.74)	0.1180	(3.00)
4-17	SR-1000	1.9975	(50.74)	0.1161	(2.95)
4-19	SR-1000	1.9971	(50.73)	0.1169	(2.97)
5-17	SR-1000	1.9937	(50.64)	0.1126	(2.86)
4-21	SR-500	1.9972	(50.73)	0.1183	(3.00)
5-3	SR-500	1.9916	(50.59)	0.1141	(2.90)
5-5	SR-500	1.9910	(50.57)	0.1132	(2.89)
5-7	SR-500	1.9902	(50.55)	0.1120	(2.84)
5-9	SR-200	1.9900	(50.55)	0.1115	(2.83)
5-11	SR-200	1.9911	(50.57)	0.1141	(2.90)
5-13	SR-100	1.9933	(50.63)	0.1152	(2.93)
5-17	SR-100	1.9937	(50.64)	0.1126	(2.86)
6-1	SR-50	1.9948	(50.67)	0.1131	(2.87)
6-3	SR-50	1.9949	(50.67)	0.1134	(2.88)
6-5	SR-20	1.9968	(50.72)	0.1147	(2.91)
6-7	SR-20	1.9958	(50.69)	0.1137	(2.89)

*In this column: ST designates a short time stress strain test; C followed by a number designates a creep test at an applied stress in ksi given by the number; SR followed by a number designates a constant strain-rate, stress-strain test at a strain rate in micro-in./in./min. given by the number.

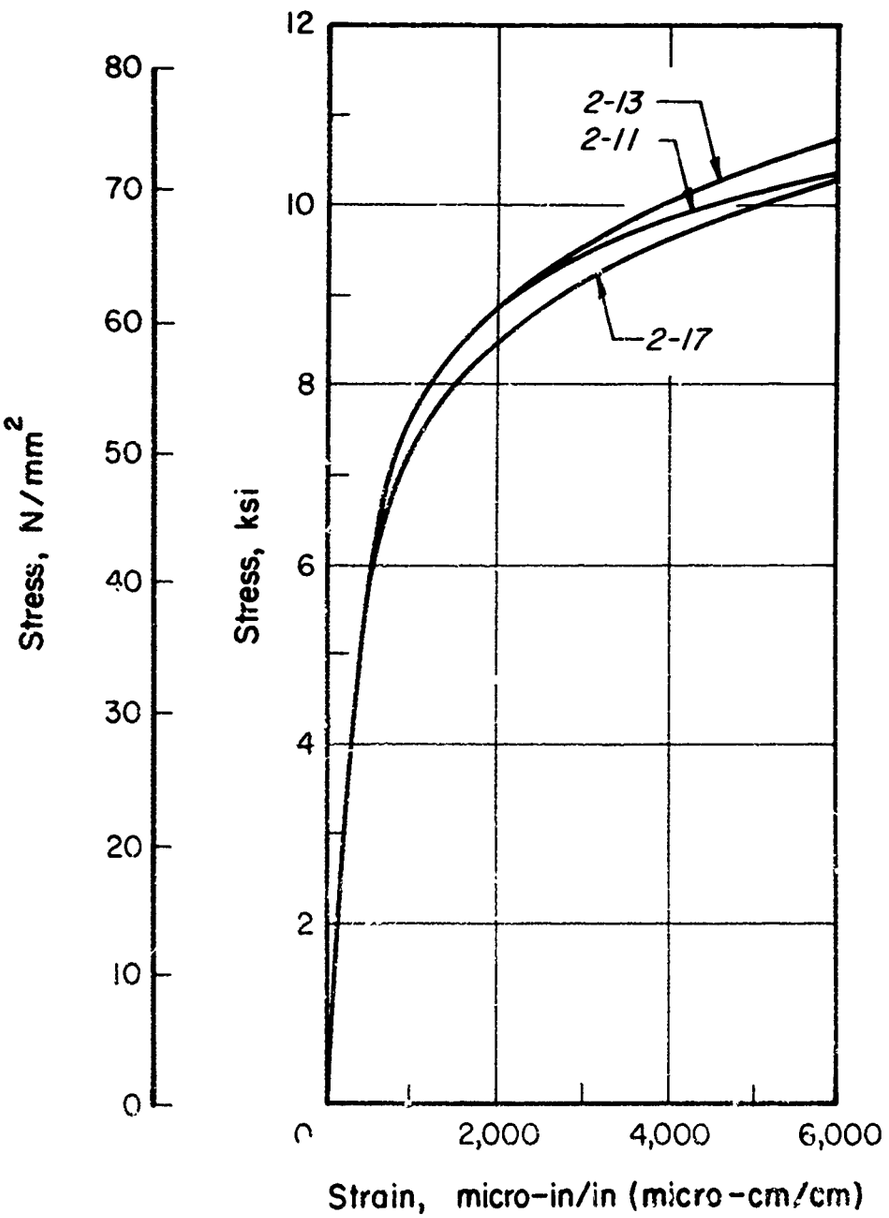

Figure 17 Constant stress-rate, short time, stress-strain curves for aluminum alloy 2024-0 at 500° F (533° K). Stress rate approximately 40,000 psi/min.

5923

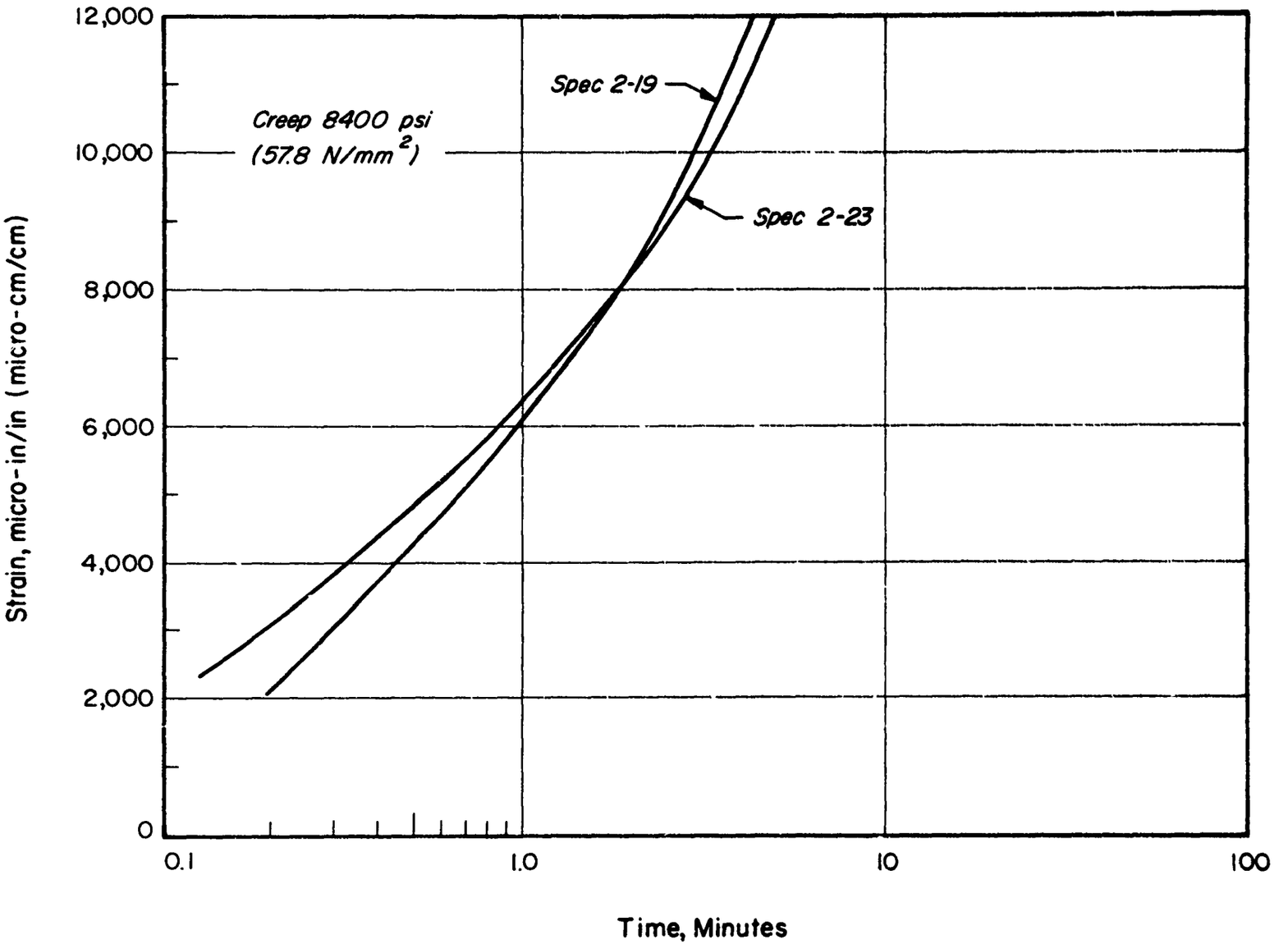

Figure 18 Creep curves at 8400 psi (57.8 N/mm^2) applied stress for aluminum alloy 2024-0 at 500° F (533° K).

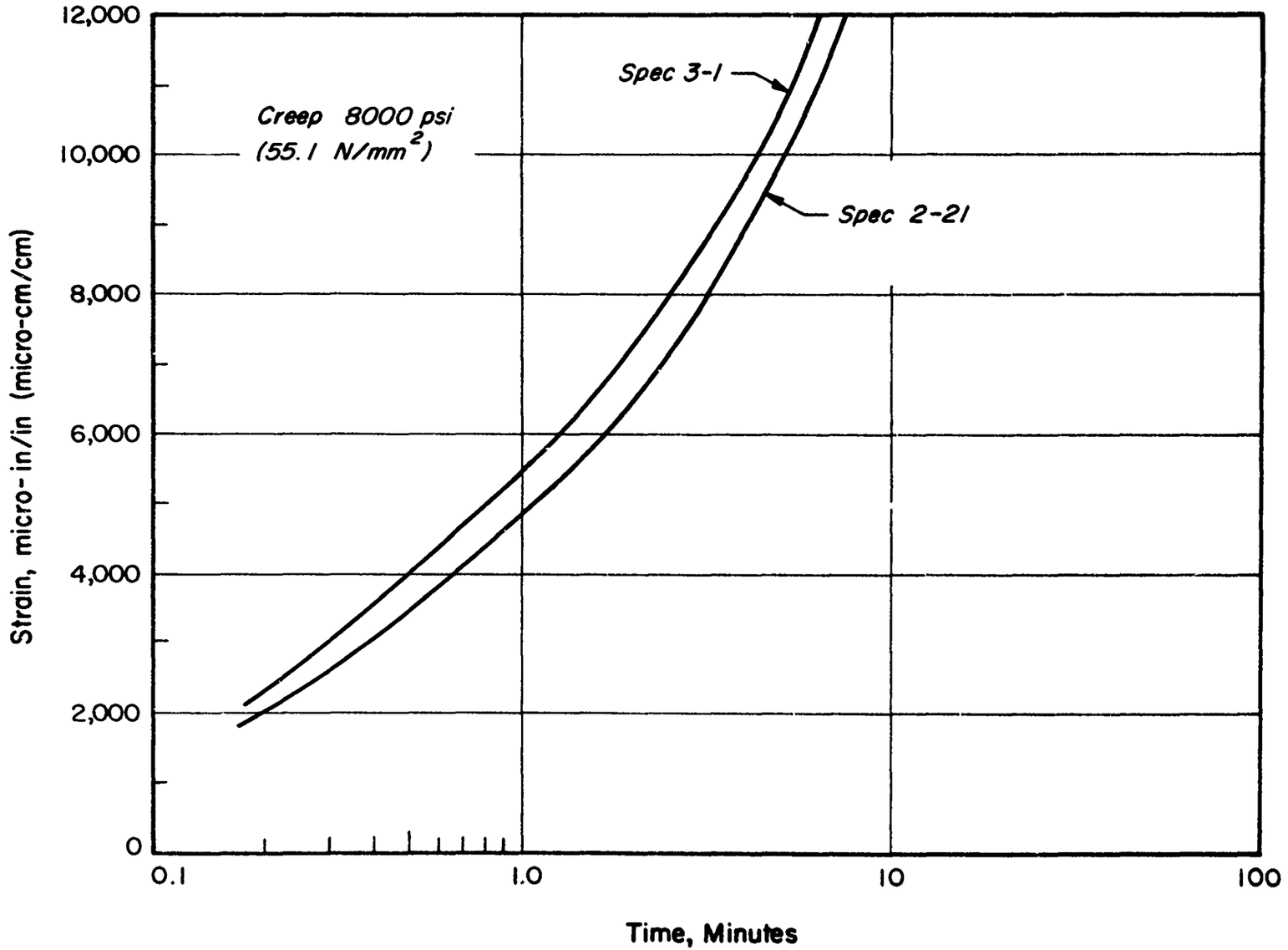

Figure 19 Creep curves at 8000 psi (55.1 N/mm²) applied stress for aluminum alloy 2024-0 at 500° F (533° K).

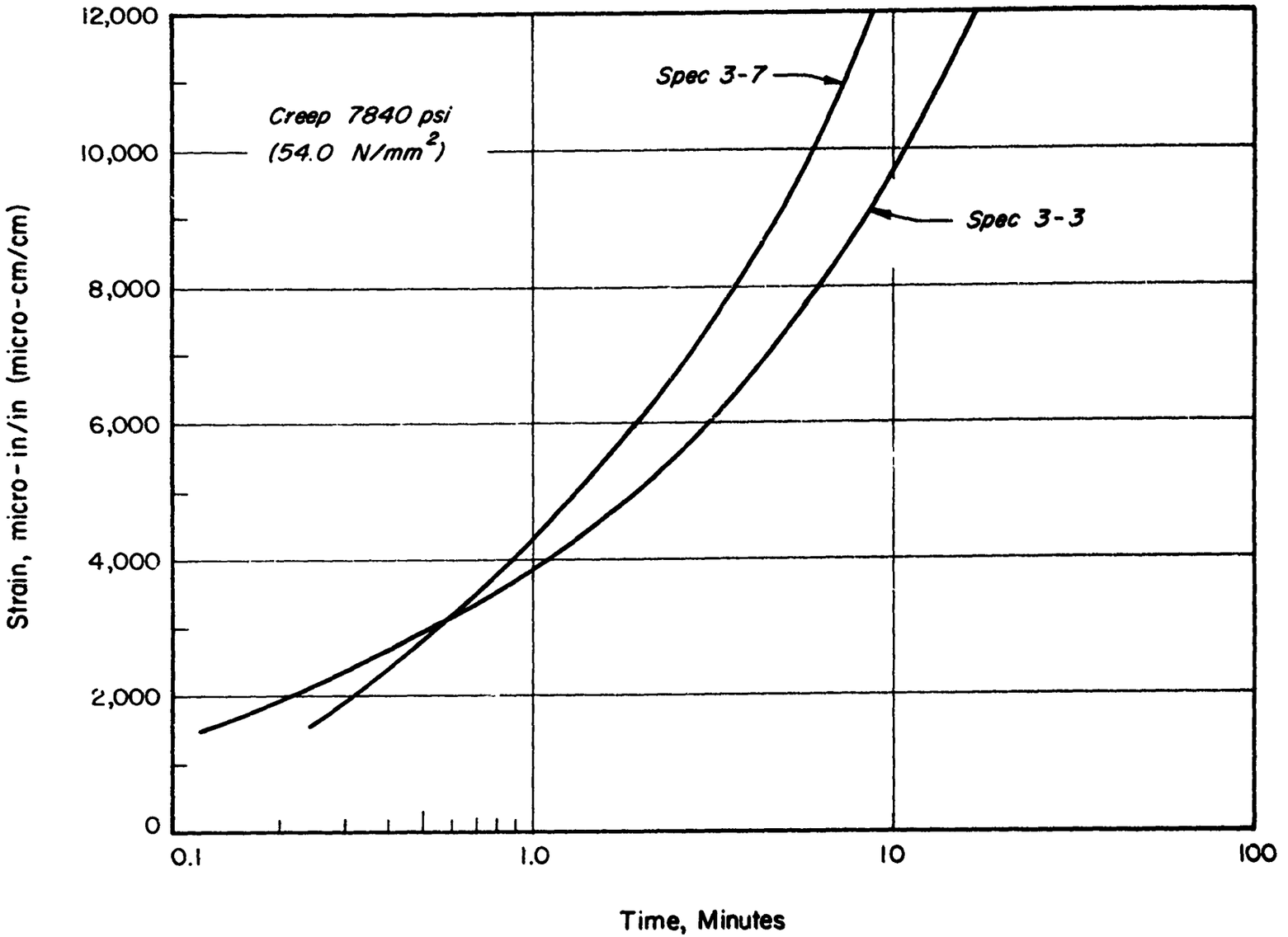

Figure 20 Creep curves at 7840 psi (54.0 N/mm²) applied stress for aluminum alloy 2024-0 at 500° F (533° K).

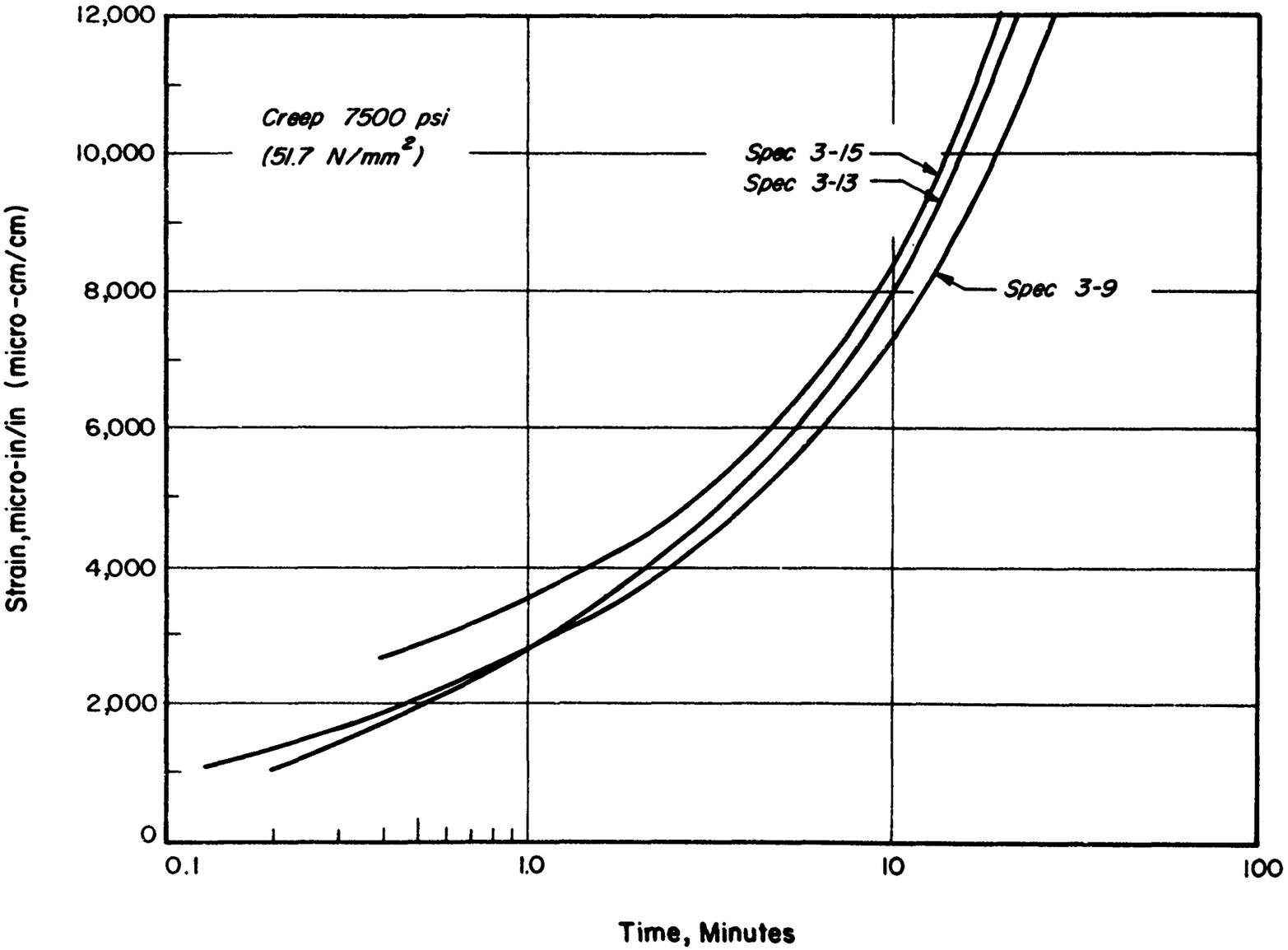

Figure 21 Creep curves at 7500 psi (51.7 N/mm²) applied stress for aluminum alloy 2024-0 at 500° F (533° K).

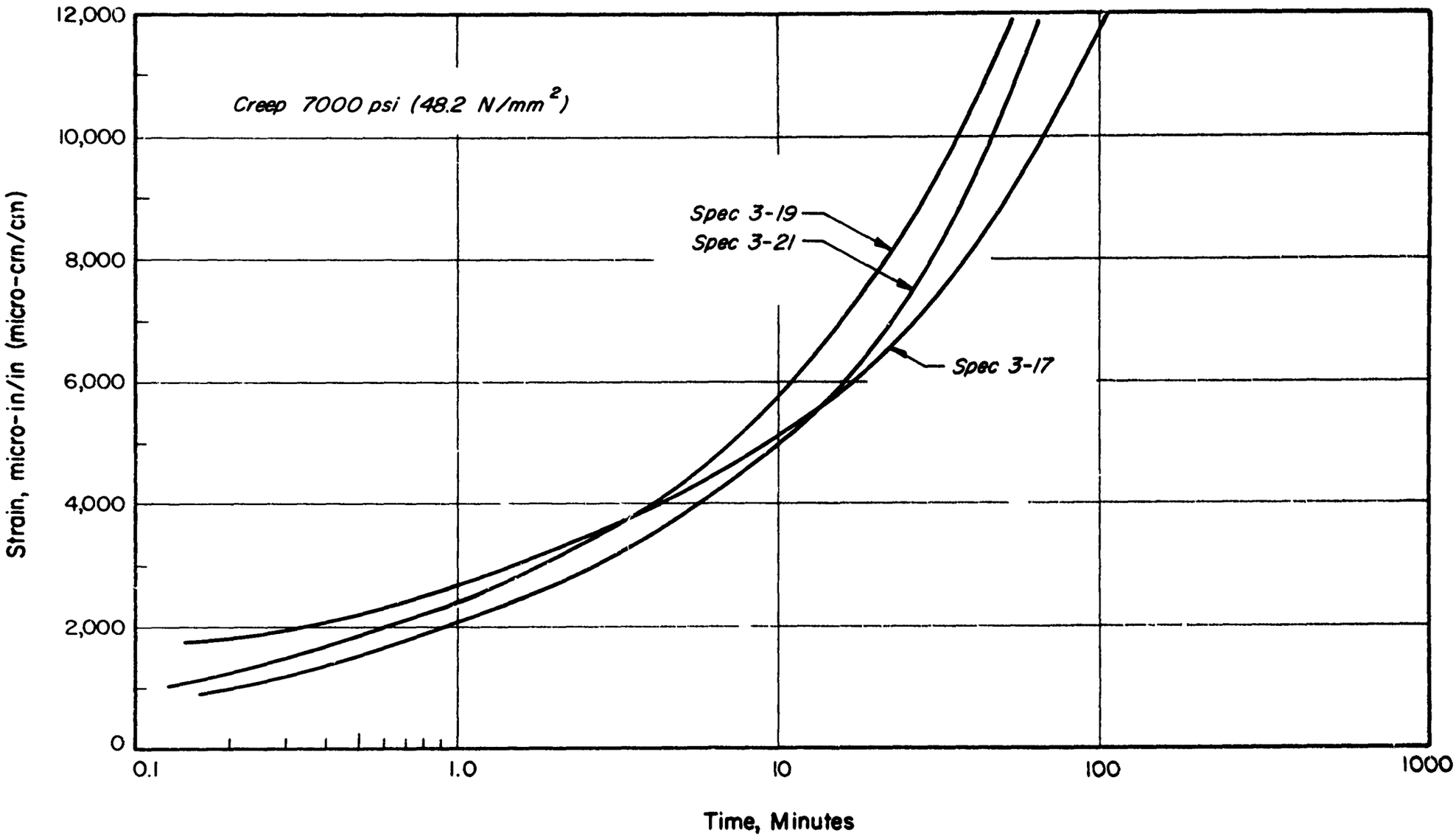

Figure 22 Creep curves at 7000 psi (43.2 N/mm²) applied stress for aluminum alloy 2024-0 at 500° F (533° K).

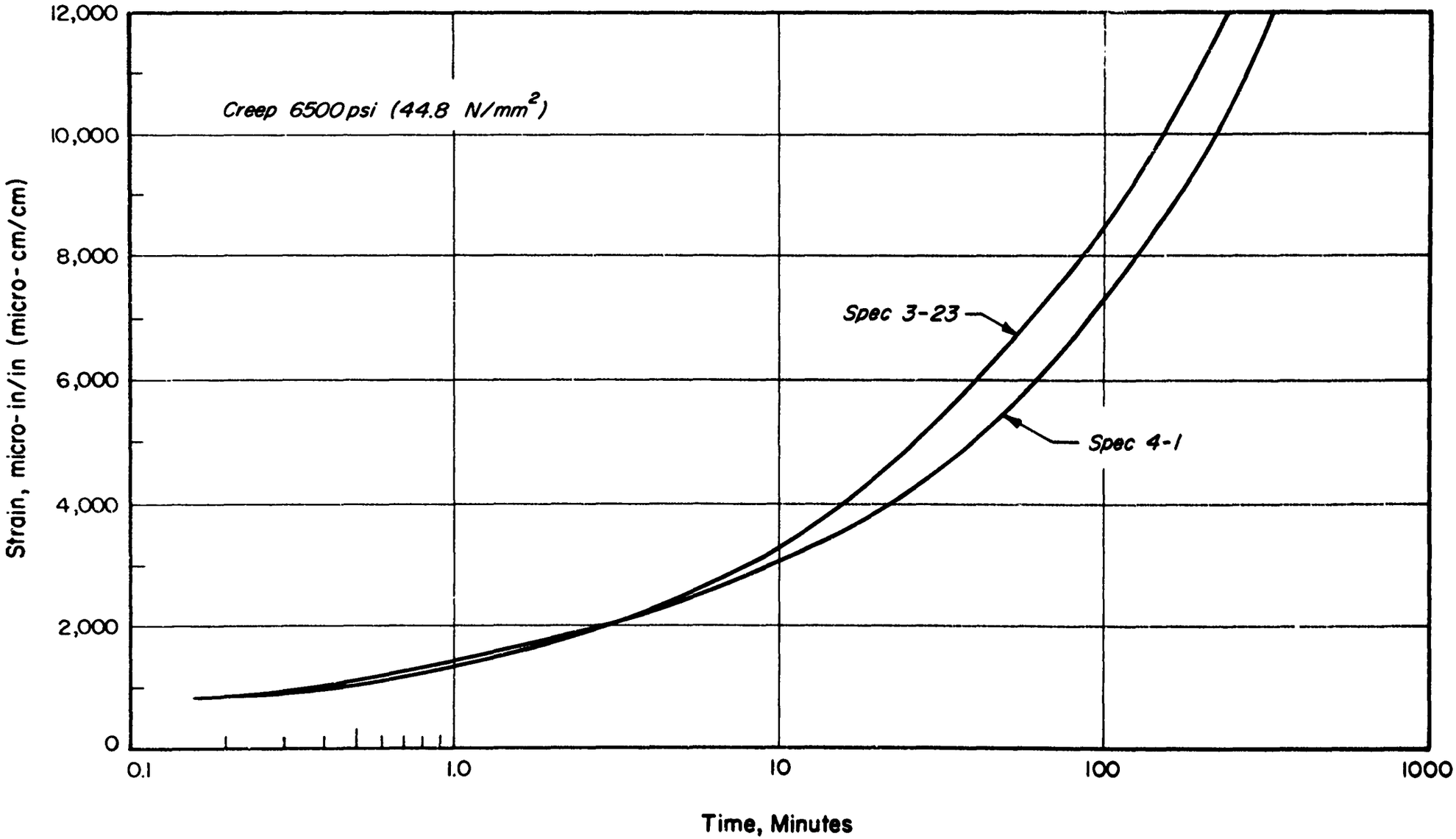

Figure 23 Creep curves at 6500 psi (44.8 N/mm²) applied stress for aluminum alloy 2024-0 at 500° F (533° K).

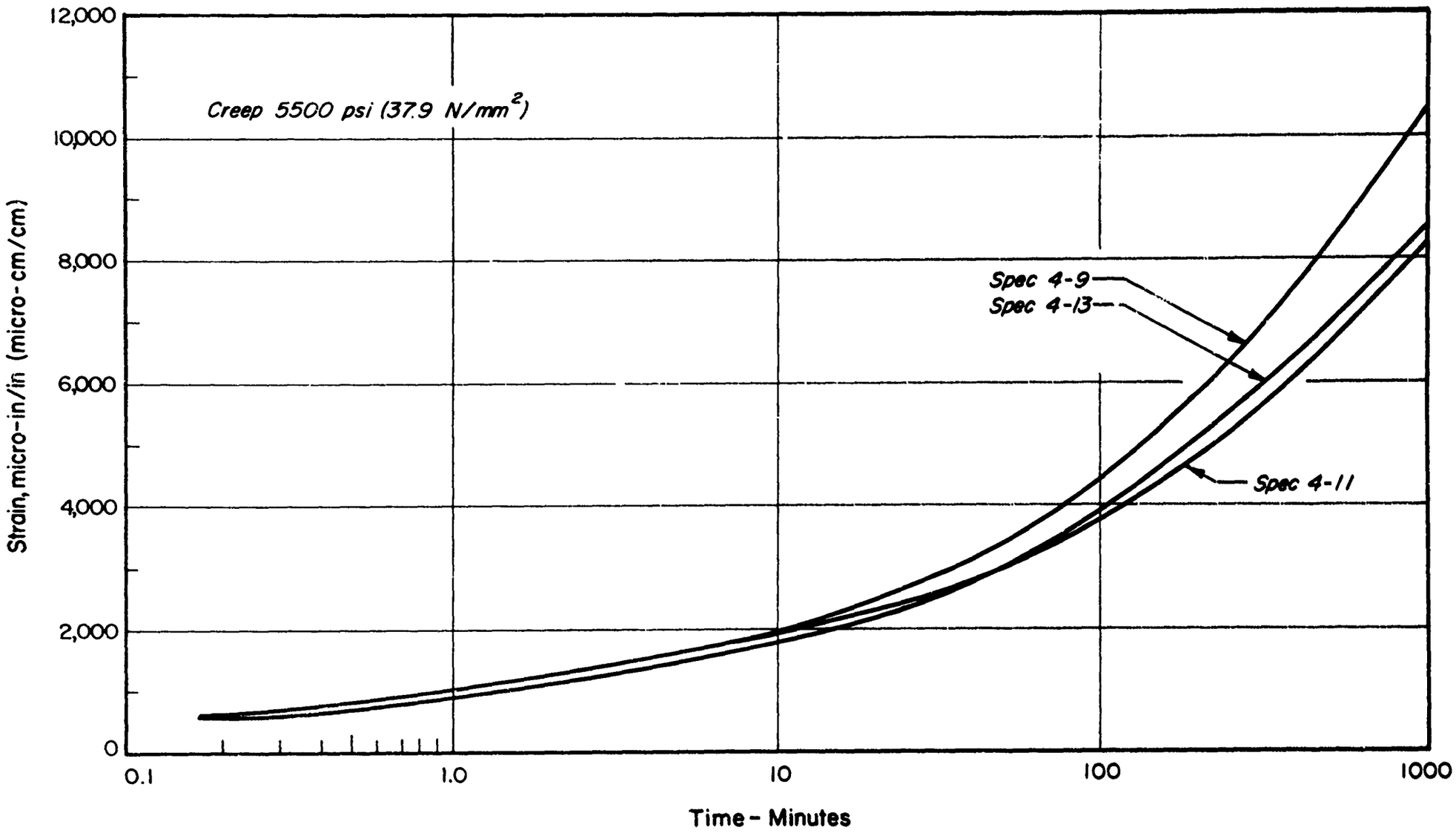

Figure 24 Creep curves at 5500 psi (37.9 N/mm²) applied stress for aluminum alloy 2024-0 at 500° F (533° K).

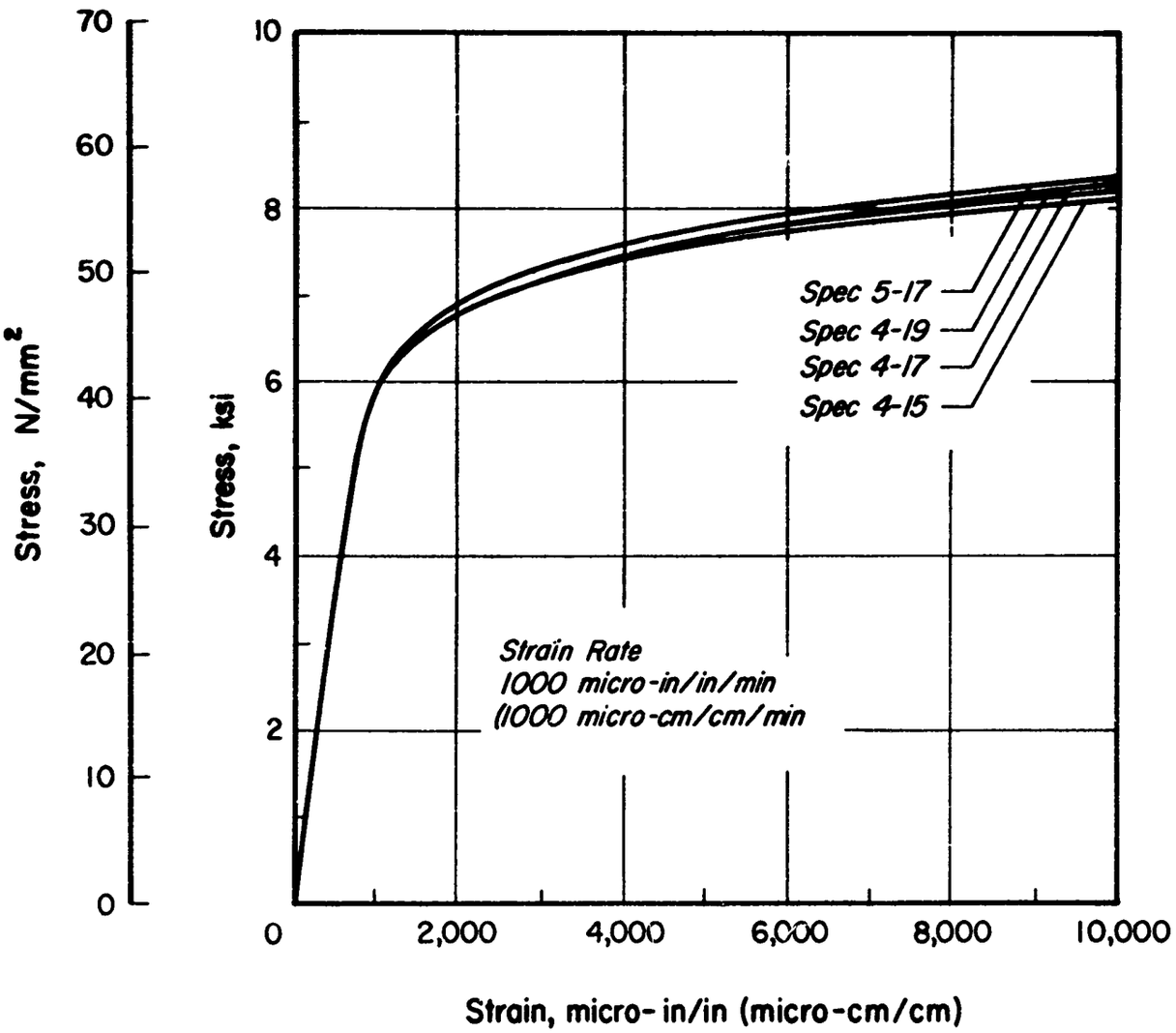

Figure 25 Constant strain-rate, stress-strain curves at 1000 micro-in/in/min (1000 micro-cm/cm/min) for aluminum alloy 2024-0 at 500° F (533° K).

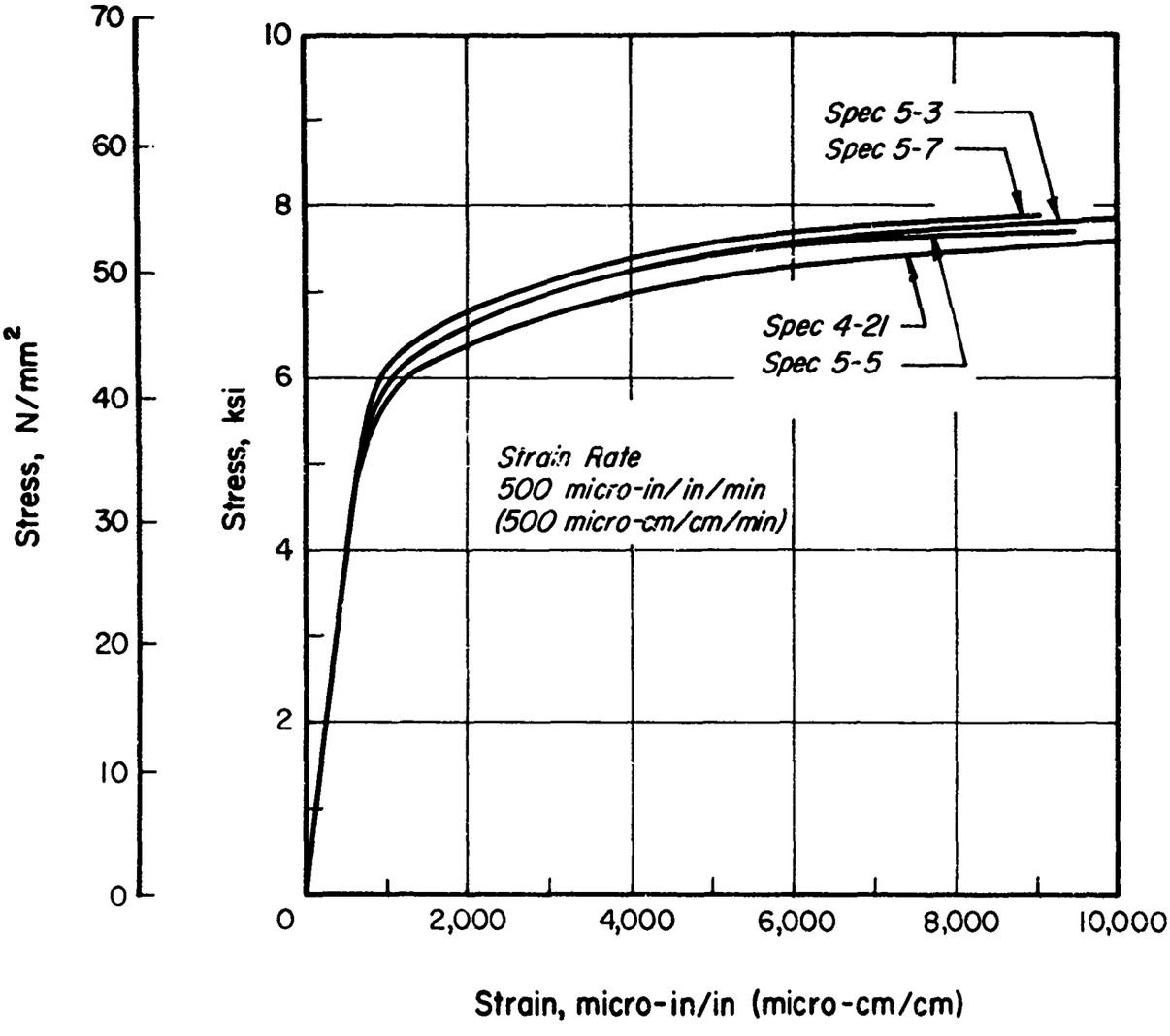

Figure 26 Constant strain-rate, stress-strain curves at 500 micro-in/in/min (500 micro-cm/cm/min) for aluminum alloy 2024-0 at 500° F (533° K).

5937

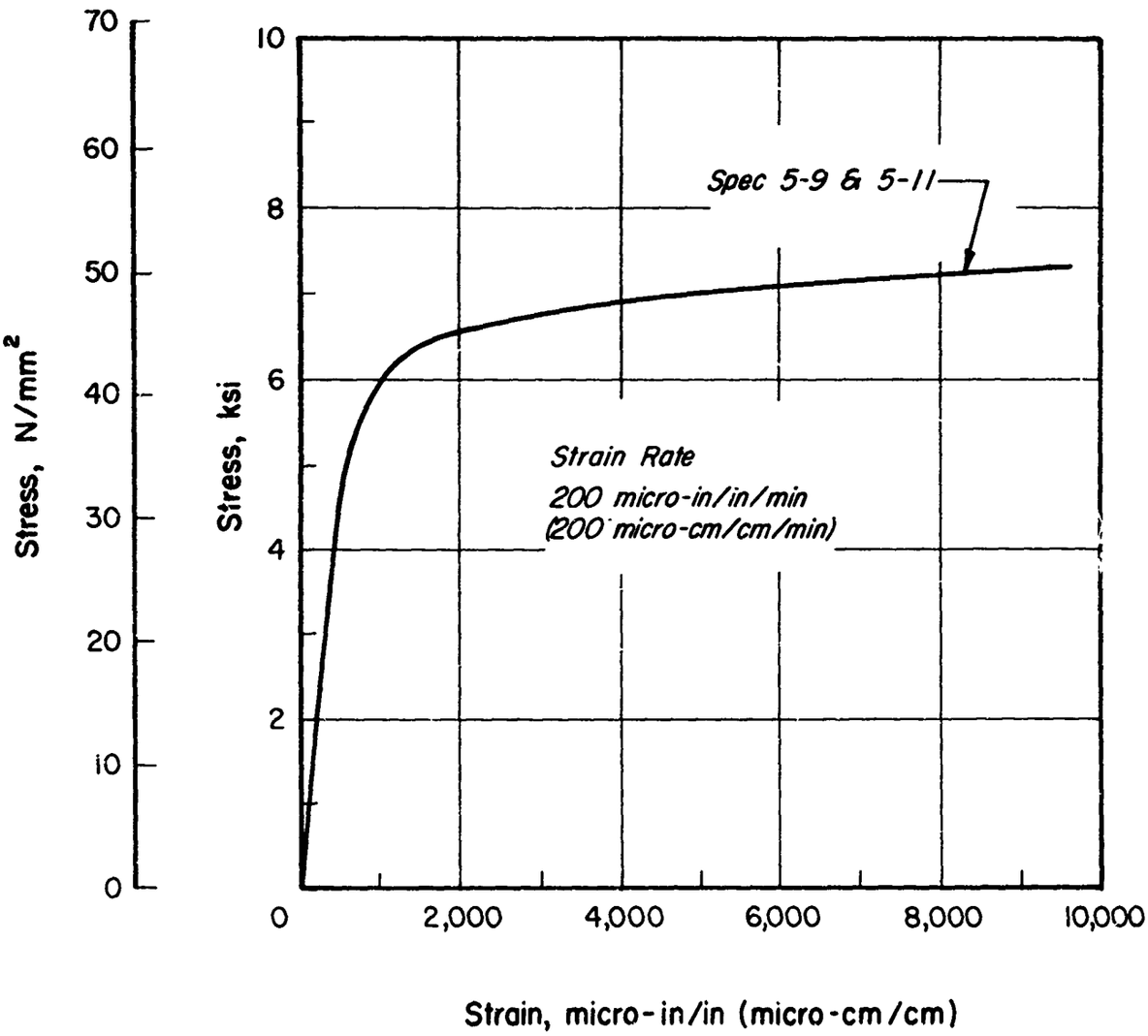

Figure 27 Constant strain-rate, stress-strain curves at 200 micro-in/in/min (200 micro-cm/cm/min) for aluminum alloy 2024-0 at 500° F (533° K).

5936

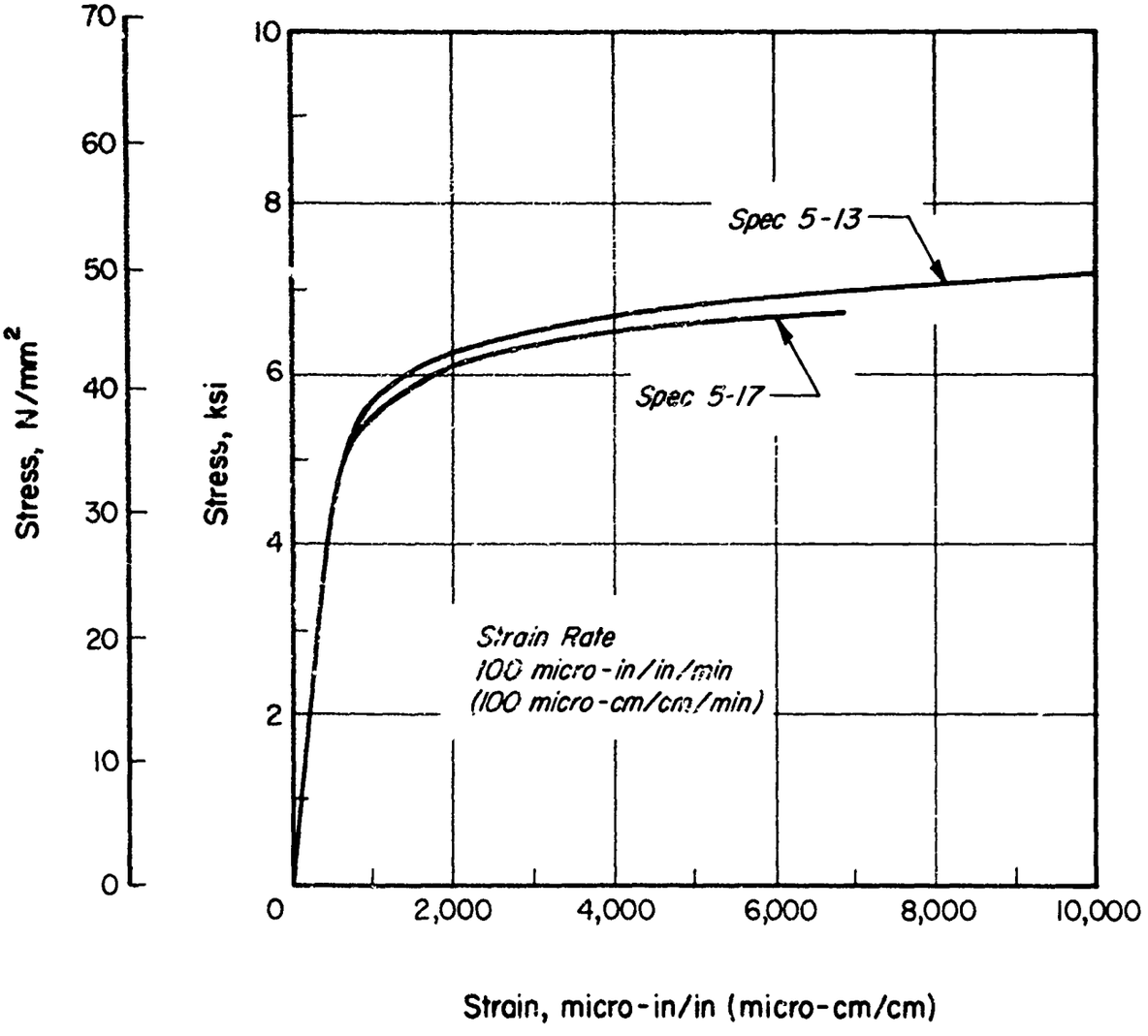

Figure 28 Constant strain-rate, stress-strain curves at 100 micro-in/in/min (100 micro-cm/cm/min) for aluminum alloy 2024-0 at 500° F (533° K).

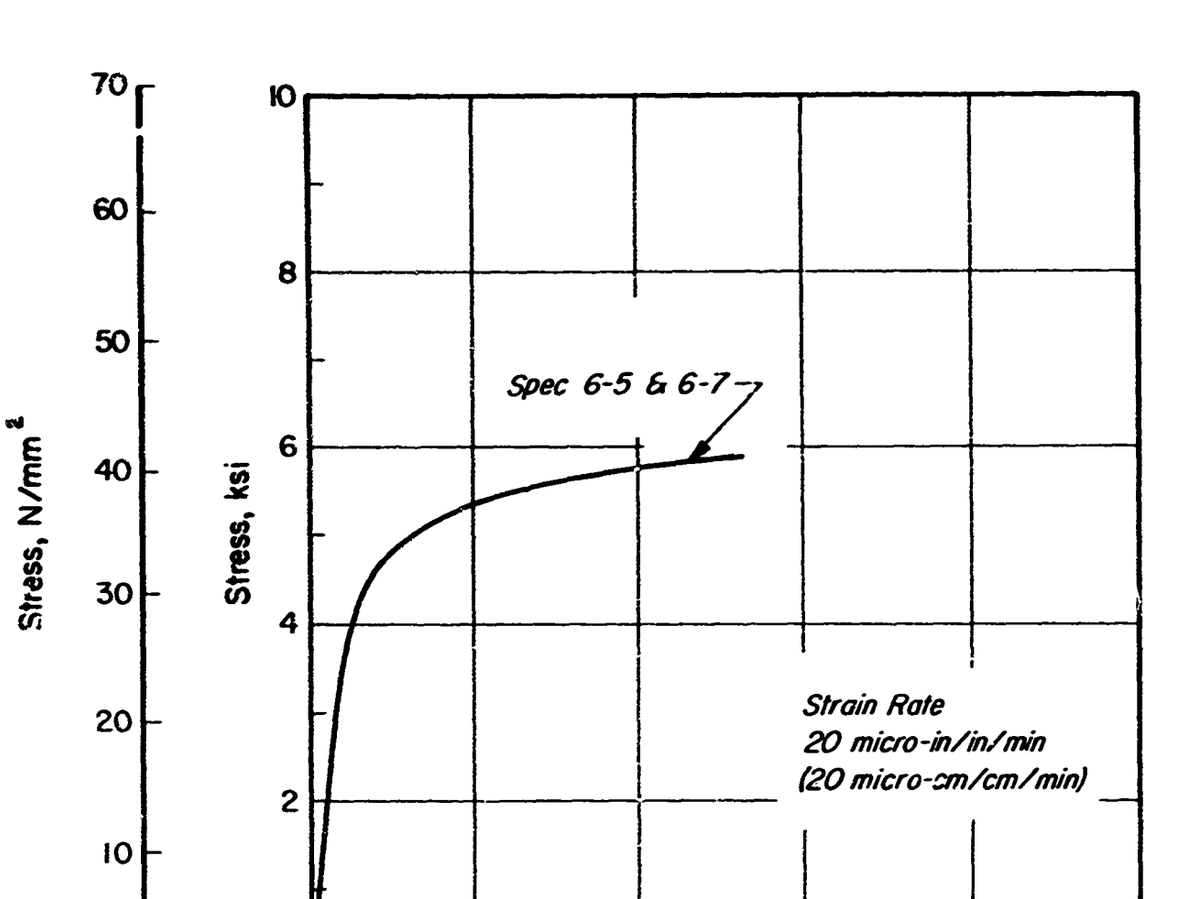

Figure 30 Constant strain-rate, stress-strain curves at 20 micro-in/in/min (20 micro-cm/cm/min) for aluminum alloy 2024-0 at 500° F (533° K).

Unclassified

Security Classification

DOCUMENT CONTROL DATA - R&D

(Security classification of title, body of abstract and indexing annotation must be entered when the overall report is classified)

1. ORIGINATING ACTIVITY (Corporate author)	2a. REPORT SECURITY CLASSIFICATION
Allied Research Associates, Inc.	Unclassified
	2b GROUP NA

3 REPORT TITLE

TIME-DEPENDENT COMPRESSION PROPERTIES OF ALUMINUM ALLOY 2024-0 at 500F (533K)

4 DESCRIPTIVE NOTES (Type of report and inclusive dates)

Technical Report - 31 October 1966

5 AUTHOR(S) (Last name, first name, initial)

Papirno, Ralph

6 REPORT DATE	7a TOTAL NO. OF PAGES	7b. NO. OF REFS
31 October 1966	43	8

8a. CONTRACT OR GRANT NO.	9a. ORIGINATOR'S REPORT NUMBER(S)
DA-31-124-ARO-D-337	ARA-290-4
b. PROJECT NO. 20014501B33G	
c.	9b. OTHER REPORT NO(S) (Any other numbers that may be assigned this report)
d.	5469.1

10 AVAILABILITY/LIMITATION NOTICES

Distribution of this document is unlimited.

The findings in this report are not to be construed as an official Department of the Army position, unless so designated by other authorized documents.

11 SUPPLEMENTARY NOTES	12. SPONSORING MILITARY ACTIVITY
None	U. S. Army Research Office-Durham Box CM, Duke Station Durham, North Carolina 27706

13 ABSTRACT

Compression creep and compression constant strain-rate tests were performed on thick wall cylindrical specimens of aluminum alloy 2024-0 at 500F (533K). Using the assumption that the equation of state of the material is a function only of stress, strain, and strain rate, the creep curves were analyzed to yield constant strain-rate, stress strain data. Comparisons between the creep-derived and the directly measured constant strain-rate data show that the data are not exactly equivalent but the discrepancies are sufficiently small so that to a first approximation the equation of state assumption can be considered valid. The data presented will be utilized in the next state of the investigation, to develop theoretical results for the Gerard Theory of Time Dependent Plastic Stability for comparison with experiments now in progress.

Key Words

Aluminum Alloys
Creep
Strain-rate Effects
Plastic Stability
Plastic Buckling

DD FORM 1 JAN 64 1473